

T H E U N I V E R S I T Y O F M I C H I G A N

COLLEGE OF ENGINEERING
Department of Electrical Engineering
Space Physics Research Laboratory

Instrumentation Report

DESIGN OF A RADIOACTIVE IONIZATION GAUGE
FOR UPPER ATMOSPHERE MEASUREMENTS

Prepared on behalf of the project by

P. O. Handy

ORA Project 05776

under contract with:

NATIONAL AERONAUTICS AND SPACE ADMINISTRATION
GODDARD SPACE FLIGHT CENTER
CONTRACT NO. NAS5-3335
GREENBELT, MARYLAND

administered through:

OFFICE OF RESEARCH ADMINISTRATION ANN ARBOR

February 1970

TABLE OF CONTENTS

	Page
LIST OF FIGURES	iv
1. INTRODUCTION	1
2. GAUGE REQUIREMENTS	2
3. RADIOACTIVE SOURCE SELECTION	3
4. MEASUREMENTS OF AMERICIUM-241 FOIL	5
4.1. Ion Current Measurements	5
4.2. Radiation Intensity Measurements	6
5. GAUGE CONSTRUCTION	8
6. GAUGE CHARACTERISTICS	13
6.1. Cylindrical Ionization Chamber	13
6.1.1. Effect of operating potentials on ion current	13
6.1.2. Ion current characteristics	17
6.1.3. Residual current at "zero" pressure	21
6.2. Planar Ionization Chamber	23
6.2.1. Chamber design	23
6.2.2. Effects of various cylinder potentials	24
6.2.3. Ion current characteristics (planar chamber)	28
7. GAUGE OPERATION	30
8. GAUGE PERFORMANCE	32
8.1. Linearity	32
8.2. Long Term Stability	32
8.3. Temperature Effects	34
8.4. Hysteresis	35
9. CONCLUSIONS	37
10. REFERENCES	38
APPENDIX A—ION CURRENT DETECTOR	39
APPENDIX B—VACUUM SYSTEM	42

LIST OF FIGURES

Figure	Page
1. Foil cross section.	5
2. Ion current vs. overcoat thickness.	6
3. Radiation intensity vs. overcoat thickness.	7
4. Gauge assembly.	10
5. Active surface pattern, Americium-241 source.	10
6. Gauge body, polarization cylinder, radioactive source and header assembly, and Teflon seal.	11
7. Assembled prototype gauge and associated electronics.	12
8. Cylindrical chamber characteristics, $P = 10, 1, \text{ and } 10^{-1}$ torr.	14
9. Cylindrical chamber characteristics, $P = 10^{-2}, 10^{-3}, \text{ and } "0"$ torr.	15
10. Potential distribution within the ionization chamber.	16
11. Summary, cylindrical chamber characteristics.	18
12. Effect of polarization potential (energetic electron region).	12
13. Residual current vs. source activity and vs. collector surface area.	22
14. Planar chamber configuration.	23
15. Potential variation with and without ion repeller.	24
16. Planar chamber characteristics, $P = 10, 100, \text{ and } 1000$ torr.	25
17. Planar chamber potential distribution.	27
18. Summary, planar chamber characteristics.	29
19. Dual collector gauge operating region, ion current vs. pressure.	31

LIST OF FIGURES (Concluded)

Figure	Page
20. Gauge nonlinearity, both chambers.	33
21. Temperature test setup.	34
22. Percent ion current change vs. temperature for constant gas density.	35
23. Electrometer amplifier block diagram.	40
24. Electrometer amplifier switching sequence.	41
25. Vacuum system and calibration control console.	43
26. Vacuum system.	44
27. Calibration control console.	45
28. Vacuum system control panel.	46

1. INTRODUCTION

During the last decade, increased knowledge of the earth's atmosphere has been due largely to the use of a variety of successful measurement techniques. With this increased knowledge, the necessity for basic measurement accuracy is generally accepted as being fundamental for a further understanding of the physical processes and the dynamics of the atmosphere. Hence, the development of new and improved measurement sensors and associated instrumentation continues to be a basic requirement for upper atmosphere research.

To date, soundings of the atmosphere up to altitudes of 30 to 35 km have been made and continue on a widespread synoptic basis by means of the balloon radiosonde which has been very successful due to its simplicity and low cost. At present, however, the neutral properties of the atmosphere in the region above 30 km up to orbital altitudes can be effectively monitored only by the use of sounding rocket techniques.

The pitot probe technique (Ainsworth, Fox, and LaGow, 1961; Simmons, 1964), which has been used by the Space Physics Research Laboratory of The University of Michigan, requires a measurement of the total gas pressure at the stagnation point on a sounding probe. Since the atmosphere up to altitudes of about 100 km is thoroughly mixed due to turbulence and convection, the need for an accurate total pressure gauge is quite evident.

The gauge that inherently possesses several desirable features and is particularly well-suited for application on sounding rockets in the 30- to 100-km altitude region is the radioactive ionization gauge. This gauge is similar to other types of ionization gauges in that it has a source of particles which cause ionization of the gas molecules. However, instead of a large number of low energy electrons employed as the ionizing agent, a small number of high energy particles emitted from a radioactive source are utilized. The positive ions created in the ionization process are then sensed on a collecting probe. This collected ion current is related to a wide range of neutral gas pressures.

Several reports describing radioactive ionization gauges have been published. A theoretical and experimental investigation of these gauges has been made by El-Moslimany (1960). Most of his work was concerned with understanding ion-ion recombination effects in an effort to extend the dynamic range of these gauges. Vacca (1956) also experimentally investigated these gauges and optimized the linear response of the Alphatron by adjusting its operating parameters. For operation over a wide dynamic range the Alphatron employs two radioactive sources in two separate chambers. Other investigations of radioactive ionization gauges have been published (Downing and Mellen, 1946; Spencer, Boggess, Brace, and El-Moslimany, 1958).

2. GAUGE REQUIREMENTS

For application in the 30- to 100-km region of the atmosphere, the ionization gauge on board sounding rockets is required to have a pressure-measuring capability over the wide dynamic range of approximately 1000 to 1×10^{-3} torr. For the accuracies guardedly acknowledged, stable, repeatable measurements demanded of the gauge were absolute requirements which proved difficult and time-consuming to attain.

For use on sounding rockets, the gauges must also fulfill other design criteria. The gauges must withstand the experienced acceleration and vibration during the thrusting phase of the rockets and subsequently must perform their intended function. Because sounding rocket experiments are destined for a single application, gauge reliability is, of course, of paramount importance.

The presence of radioactive material is a distinct disadvantage of this type of gauge and consequently special precautions must be imposed. Since considerable preparation both in the laboratory and in the field is necessary to ready the experiments for launch, the radioactive health hazard and contamination problems must be minimized.

3. RADIOACTIVE SOURCE SELECTION

Initially radioactive tritium, which is a low energy beta emitter, was selected as the ionizing source. One reason for this choice is the less toxic or hazardous nature of tritium in comparison to other radioactive materials that yield more penetrating particles. Another factor which was considered in the choice of tritium is the electron energy loss through ionization. This is the most important process for electron energies below and about 1 MeV and varies approximately as the inverse of the electron energy. Tritium, which emits electrons with an energy of only 15 KeV (Liverhant, 1960), is therefore a very effective ionizing source.

However, the use of tritium as the ionizing source proved undesirable. Tritium in its pure form is a gas. The usable source normally contained two curies of activity of tritium which was gettered in titanium (which was previously vacuum-deposited on a stainless steel backing plate) at elevated temperatures. Consequently, considerable care was required to control the spread of contamination during the installation of the unsealed sources of relatively high activity in the gauges.

Another drawback encountered in attempting to utilize tritium as the ionizing source was in designing a mechanical configuration which would be compatible with the desired electrical configuration. In addition, the short half-life of tritium (about twelve and one-half years) was a factor influencing long-term gauge stability.

The use of tritium as the ionizing source also fixes an upper pressure measurement limit somewhat dependent on the gauge design. The limit is due to the low kinetic energy of an emitted beta particle expended in the ionization process in a relatively short pathlength at the higher pressures. When the pathlength becomes less than the dimensions of the ion chamber, a constant number of ion pairs are created. The ion current will then become independent of pressure.

One of the gauge requirements, however, was to be able to sense the higher pressures. Thus, the effects of more energetic particles emitted from a source of Americium-241 were investigated. The nuclear properties of Americium-241 (Strain and Leddicottee, 1962), that is, its half-life and radiation characteristics, were considered most favorable for this application. The 5.5 MeV alpha particles serve as an excellent ionizing source. The half-life of 462 years is sufficiently long to preclude decay corrections. The low energy gamma rays of 0.060 MeV which accompany the alpha decay, being sufficiently weak, are easily shielded.

Other important factors were considered in the selection of Americium for

this application. The sources could be fabricated in a form compatible with the electrical configuration desired in the gauge design. Preliminary information also indicated some alleviation of the contamination problems which had been previously encountered with the use of the tritium sources.

4. MEASUREMENTS OF AMERICIUM-241 FOIL

A number of test samples of Americium-241 impregnated foils were manufactured by United States Radium Corporation (now supplied by Nuclear Radiation Developments, Inc., a subsidiary of Electronics Associates of Canada, Ltd.) with varying activity content and sealing overcoat thickness. The characteristics of the test samples are listed below. Figure 1 shows the foil cross section.

Sample Number	Activity (mc/in ²)	Sample Size (in.)	Au Overcoat (μ)	Active Thickness (μ)
A-1	8.35	1/2 x 1/2	1.62	4
A-3	8.35	1/2 x 1/2	4.07	4
A-5	8.35	1/2 x 1/2	5.69	4
A-7	8.35	1/2 x 1/2	7.32	4
B-1	16.7	1/2 x 1/2	3.27	8
B-3	16.7	1/2 x 1/2	4.91	8
B-5	16.7	1/2 x 1/2	6.54	8
B-7	16.7	1/2 x 1/2	8.03	8

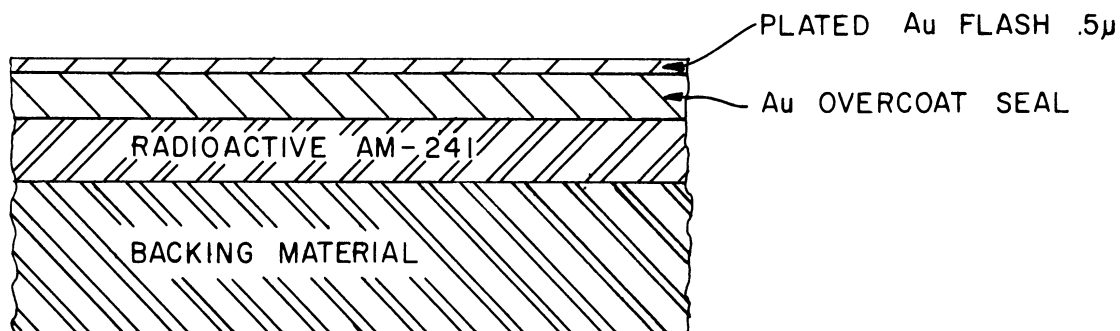


Figure 1. Foil cross section.

4.1. ION CURRENT MEASUREMENTS

Positive ion current measurements were taken with each of the samples used as the ionizing source. The ion chamber employed was a parallel-plate type air ionization chamber with a 4-in. diameter collector plate. The plate separation distance was 1.5 in., and the potential difference applied between the plates was 5000 V. At this potential the ion current measurements were

taken well into the saturated current characteristics at atmospheric pressure. The instrument used to measure the ion current was a Keithley Model 414 $\mu\mu$ ammeter.

The results of these measurements are shown in Figure 2. The effective ionizing strength of a source for a given activity is greater with reduced gold overcoat thickness. Note that in doubling the activity of the sample, i.e., the active thickness, the effective ionizing strength for a given gold overcoat thickness does not appear to increase. The reason for this is that in the more buried portion of the active layer the alpha particles are almost completely absorbed before they can reach the surface of the foil and escape. This portion of the active layer then yields no contribution for the gas ionization.

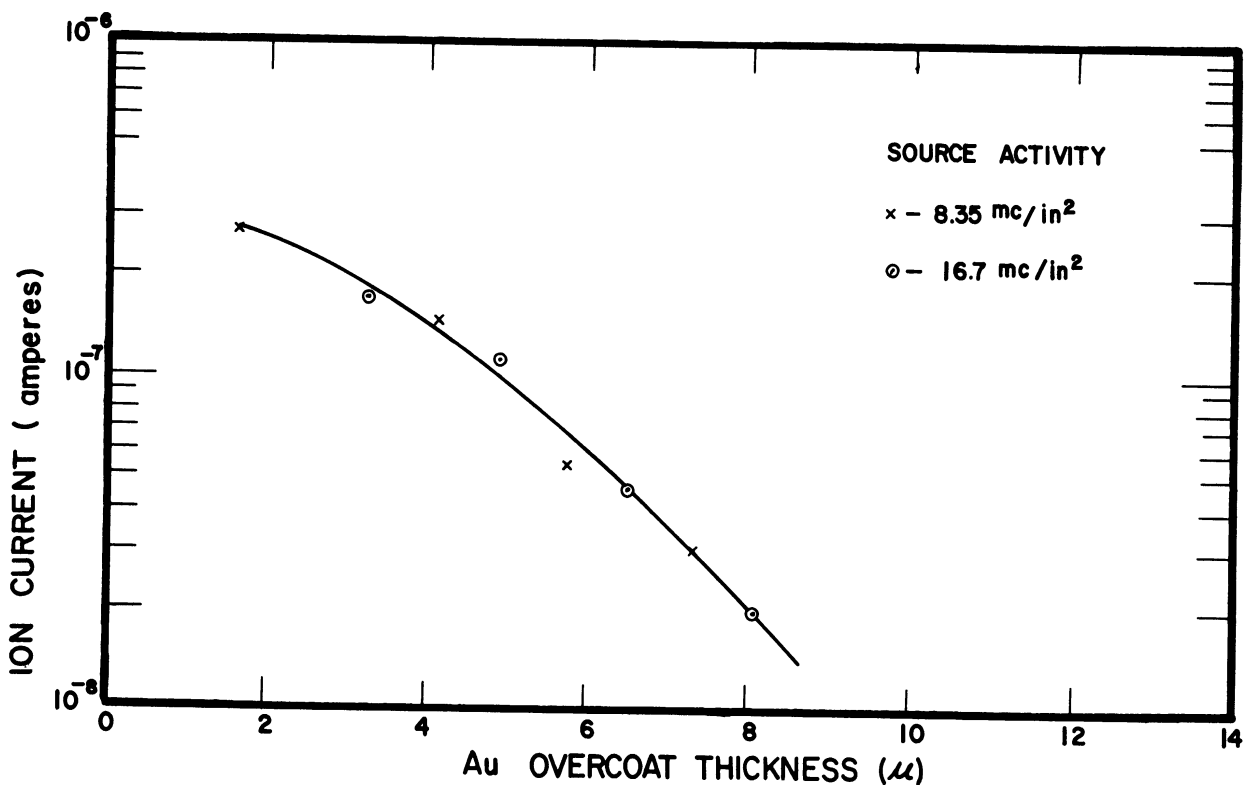


Figure 2. Ion current vs. overcoat thickness.

4.2. RADIATION INTENSITY MEASUREMENTS

The gamma output from the samples was measured by means of a Beckman Model MX-4 meter. The meter is a battery-powered instrument with a 1000-ml volume ion chamber, and was calibrated with the use of NBS certified Ra²²⁶ needles. The construction of the chamber permits windows of varying thickness to be placed over the front of the chamber. Readings were obtained from the sample foils by using each of two different windows on the meter so that calculations for air absorption could be made. One of the windows was 1.3 mg/cm² and the other was a 353 mg/cm² window.

The results shown in Figure 3 were taken at a distance of 10 cm from the meter window to the samples and are fairly low level intensities. In the manner in which the sources would be handled, the radiation intensity levels would not present a health hazard.

From the measurement results, a foil with an activity level of 8.35 mc/in.² and a gold overcoat seal 1.62 μ thick was selected for the ionizing source in the gauges. This is the minimum recommended gold overcoat thickness for a source of this activity, and results in a source with a relatively high effective ionizing strength.

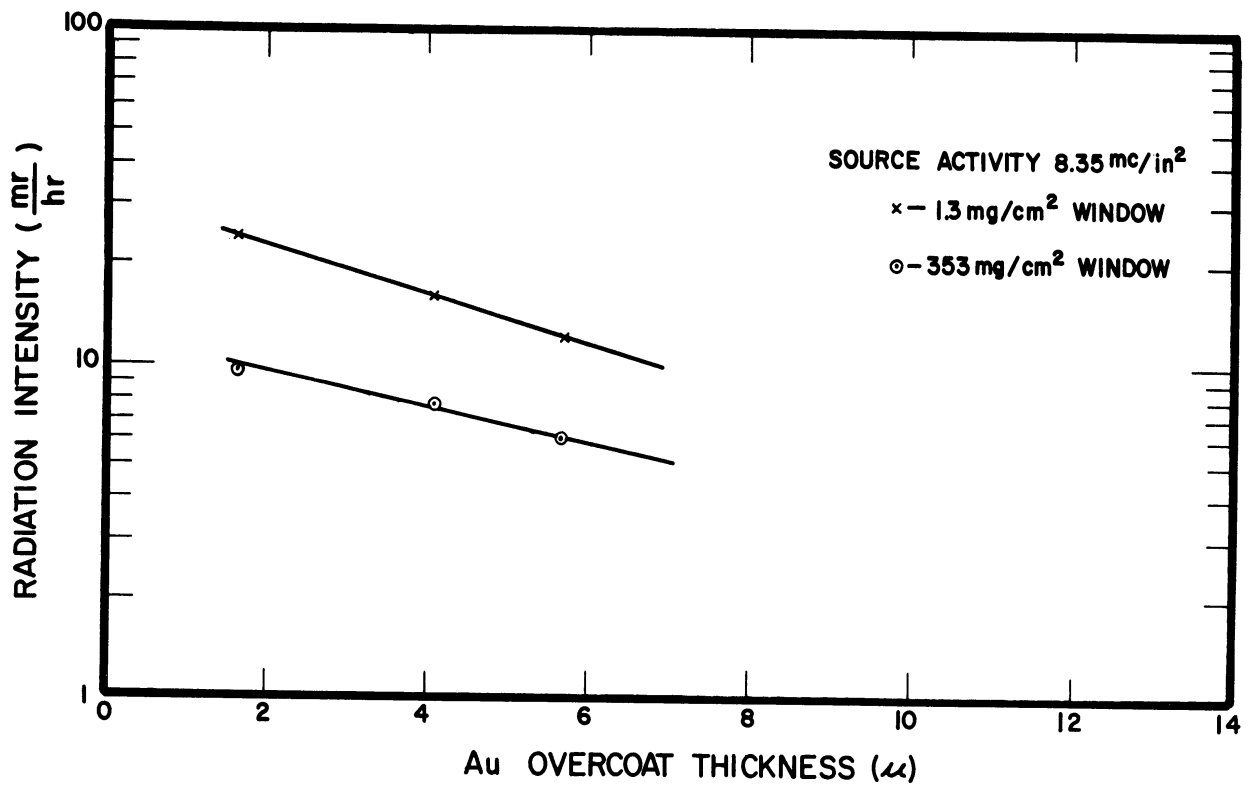


Figure 3. Radiation intensity vs. overcoat thickness.

5. GAUGE CONSTRUCTION

In the design of the gauge, attention was given to a simple, rugged construction. The mechanical assembly is shown in Figure 4a. Wherever practical, stainless steel is used. Teflon seals under compression provide the vacuum seals as well as the electrical insulation of the polarization cylinder from the gauge body. The use of ceramic to metal vacuum-sealed feedthroughs provides the high electrical impedance required for the measurement of the fairly low ion currents.

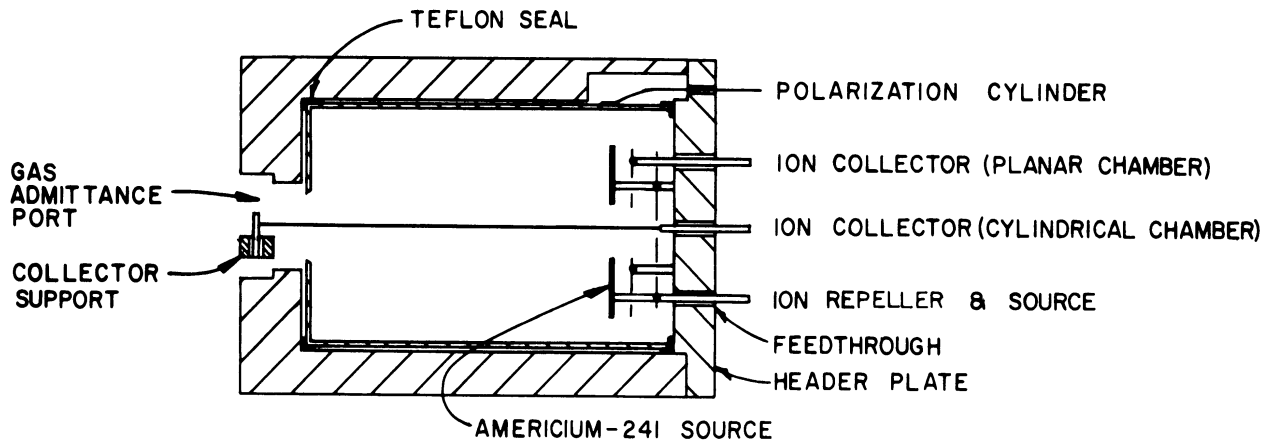
In order to obtain measurements over the desired pressure range, two ionization chambers are employed. These two chambers are shown in Figures 4b and 4c. The planar ionization chamber is designed for measurements of high pressures, and the cylindrical ionization chamber for measurements of the lower pressures. For direct emission of the alpha particles into each ionization chamber, the radioactive source is manufactured with both sides active and placed so that the two chambers can be constructed on either side of it.

From earlier efforts, which resulted in the present gauge design, a particular electrical configuration for the operation of each of the ionization chambers proved desirable. In order to duplicate these configurations, the radioactive source was mounted on feedthrough pins. For this application the source is in the form of a flat washer approximately 0.035 in. thick with an outside diameter of 0.937 in. and an inside diameter of 0.375 in. However, the active surface lies within these two dimensions, being blanked out with an outside diameter of less than 0.937 in. and an inside diameter greater than 0.375 in. as shown in Figure 5. In addition, the outside diameter is blanked in a special pattern which enables the source to be mounted to the 0.040 in. diameter feedthrough pins.

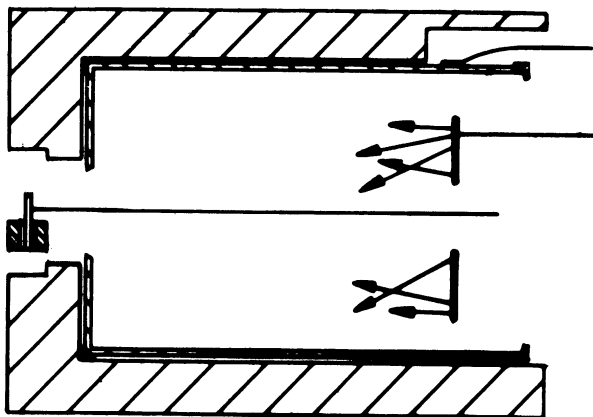
The ion collector for the cylindrical chamber is a 0.005 in. diameter stainless steel wire. The ion collector and ion repeller for the planar chamber are stainless steel screens and are spot-welded into position. The collector support is also spot-welded into position. Both feedthrough headers, i.e., the collector support and the large header, are at ground potential in order to minimize current leakage to the collectors.

An end view of an assembled prototype gauge is shown in Figure 6. The collector support for the cylindrical chamber ion collector which is spot-welded to the gauge body can be seen in front of the gas admittance port. An additional polarization chamber with a 0.005 in. diameter wire (barely visible) extending through its admittance port can also be seen, as can the radioactive source mounted on the feedthrough pins of the header assembly along with the stainless steel screens which are spot-welded into position just below the source. One of the Teflon seals used as a vacuum seal and also as an insulator for the polarization cylinder from the gauge body is shown at the right.

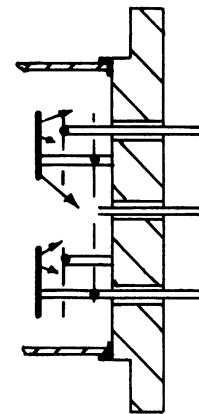
A view of the assembled prototype gauge and associated electronics (i.e., the high impedance and low impedance sections of the electrometer amplifier which is used for the ion current measurements and is described briefly in a later section, and the control unit for the amplifier) is shown in Figure 7. The sealing cover of the high impedance section of the electrometer amplifier is separated somewhat from the gauge with some of the electrical connections visible. Again, the Teflon seals, polarization cylinder, and radioactive source/header assembly for the gauge are also shown.



a) Mechanical assembly



b) Cylindrical ion chamber



c) Planar ion chamber

Figure 4. Gauge assembly.

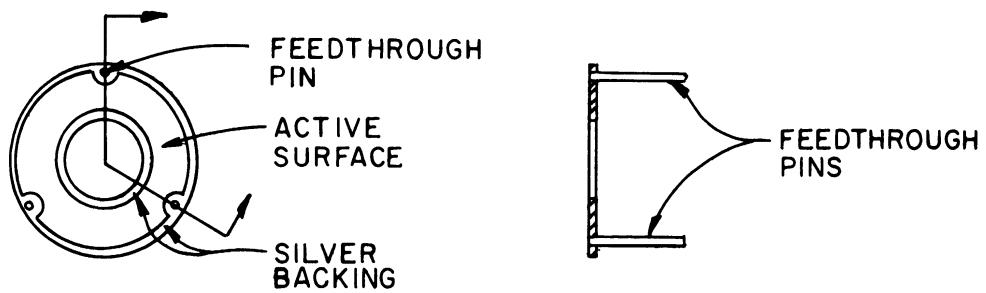


Figure 5. Active surface pattern, Americium-241 source.

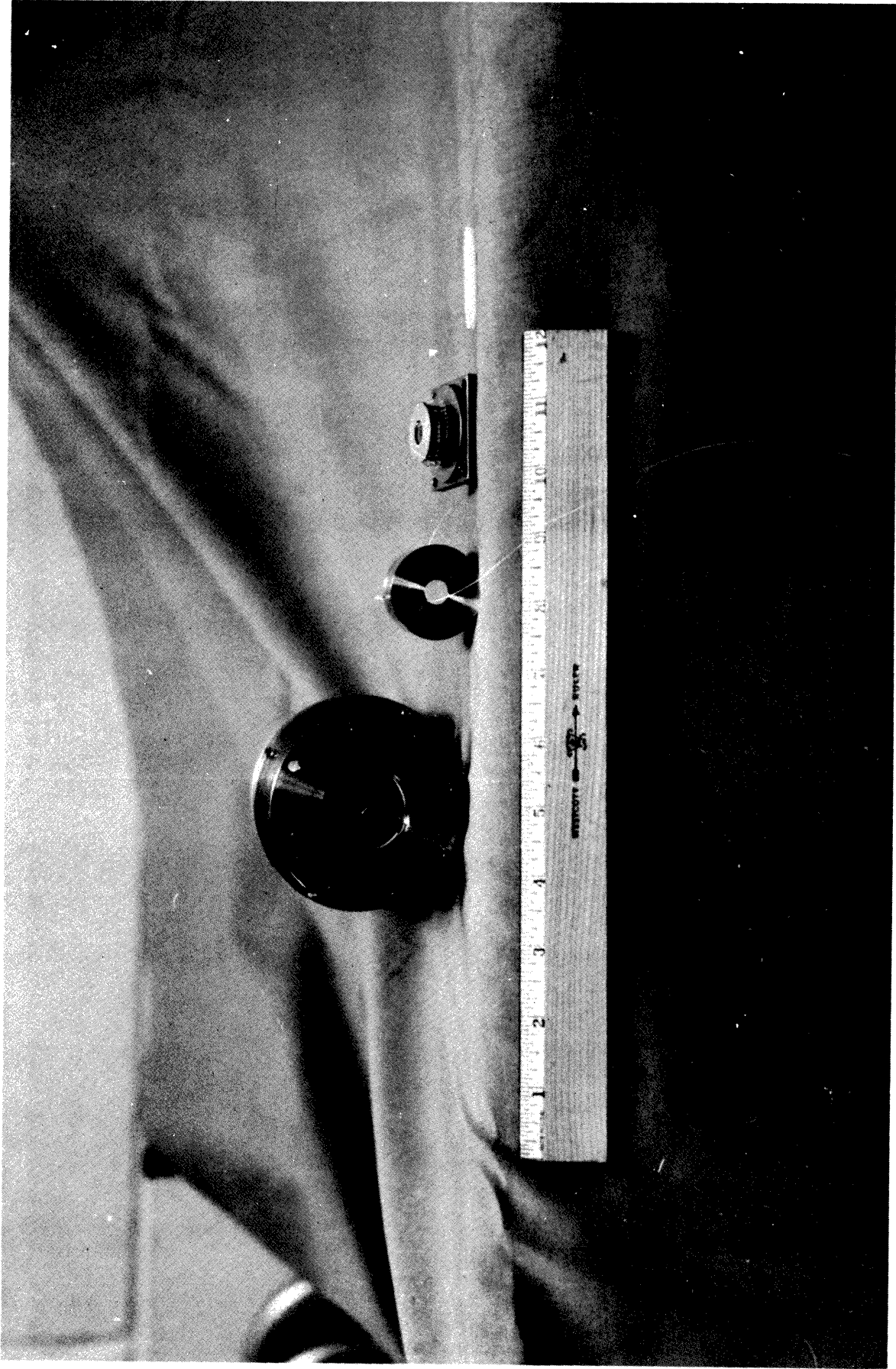


Figure 6. Gauge body, polarization cylinder, radioactive source and header assembly, and Teflon seal.

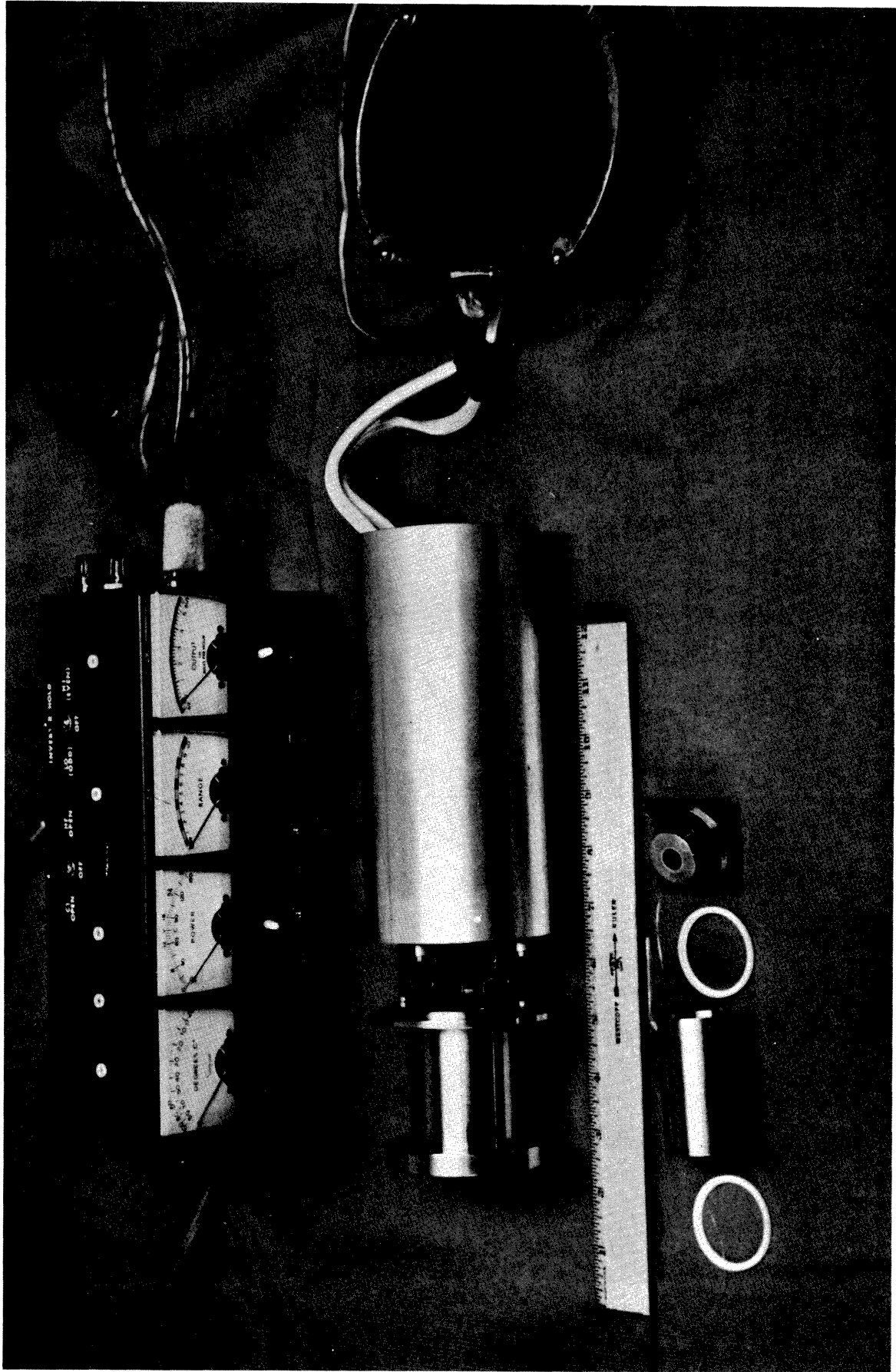


Figure 7. Assembled prototype gauge and associated electronics.

6. GAUGE CHARACTERISTICS

6.1. CYLINDRICAL IONIZATION CHAMBER

6.1.1. Effect of Operating Potentials on Ion Current

Measured positive ion current as a function of polarization cylinder potential for various pressure levels is shown in Figures 8 and 9 for three different potentials applied to the source. For operating potentials greater than approximately +20 V, the majority of the electrons and positive ions created in the ionization process are attracted to their respective collectors. For the purpose here, attention will be generally limited to this region of operation.

It is immediately apparent from the results that the ion current is highly affected by the operating potentials. Since one of the characteristics of radioactive ionization gauges is an almost uniform ionization rate throughout their entire ionization chambers, the magnitude of the measured ion current is then determined, to a large extent, for a given pressure and source activity by the size of the volume or region from which the ions are collected.

As shown in Figure 10, a collected ion boundary is set up by the potential distribution within the ionization chamber. Only those positive ions created within the volume bounded by the polarization cylinder and the collected ion boundary are attracted to the ion collector. The potential distribution, which is determined by the operating potentials, is then the controlling factor in the size of the ion collection region.

For potentials applied to the radioactive source either greater or less than the electrical potential applied to the polarization cylinder, the ion collection region is smaller in volume than the ionization chamber and quite sensitive to changes in these applied potentials. Consequently, the measured ion current is less than the total current created and is also sensitive to changes in the operating potentials.

However, these effects can be practically avoided by maintaining the polarization cylinder and the source at the same potential. For this condition, the collected ion boundary encompasses the entire ionization chamber as shown in Figure 10b. The volume from which the ions are collected is then the chamber volume, a constant, independent of the operation potential. As a result, the measured ion current becomes insensitive to changes in the operating potential (ignoring recombination effects, field intensified ionization effects, etc., which will be discussed later). In addition, the ion current magnitude is also a maximum for a given pressure.

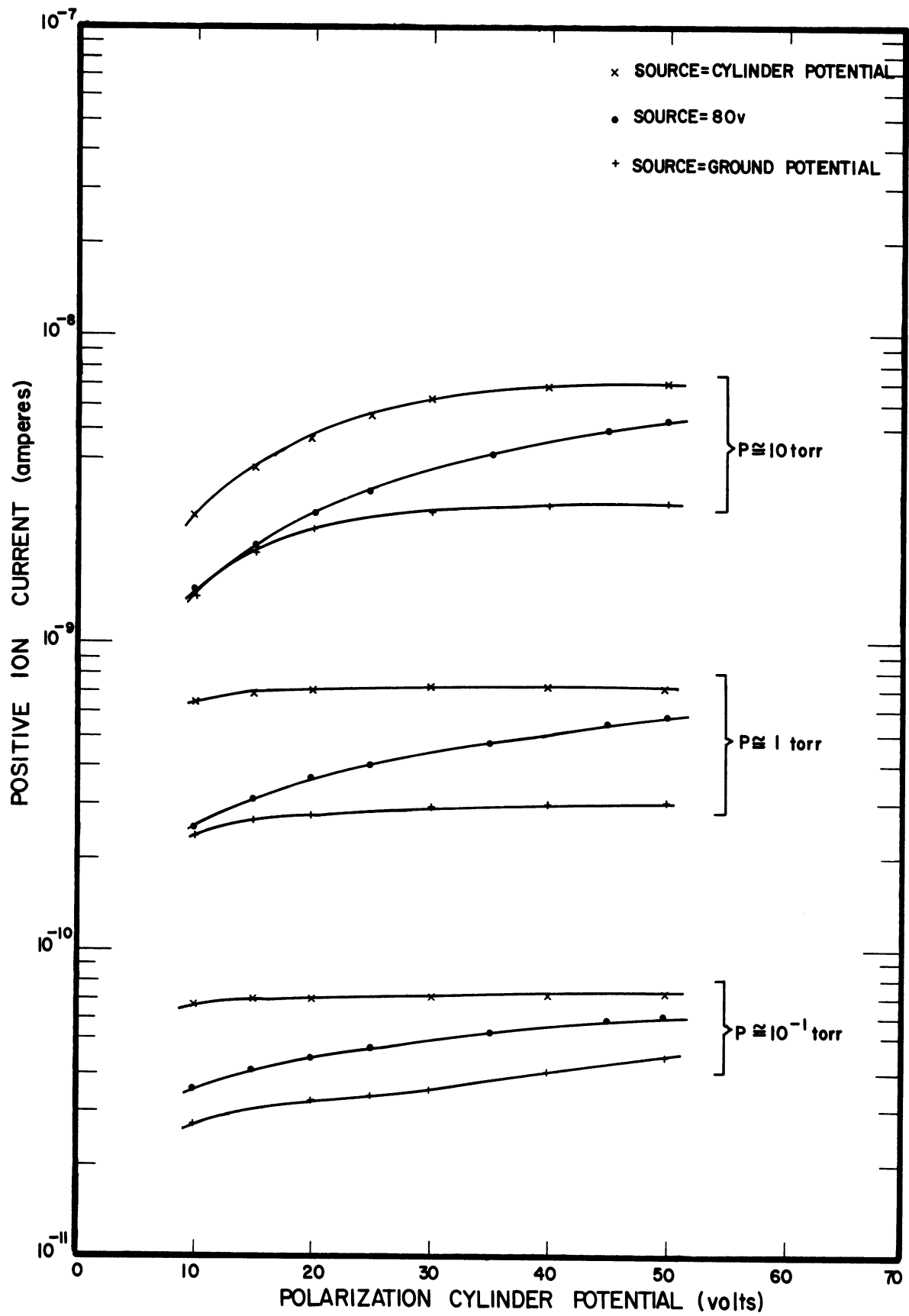


Figure 8. Cylindrical chamber characteristics, $P = 10, 1, \text{ and } 10^{-1}$ torr.

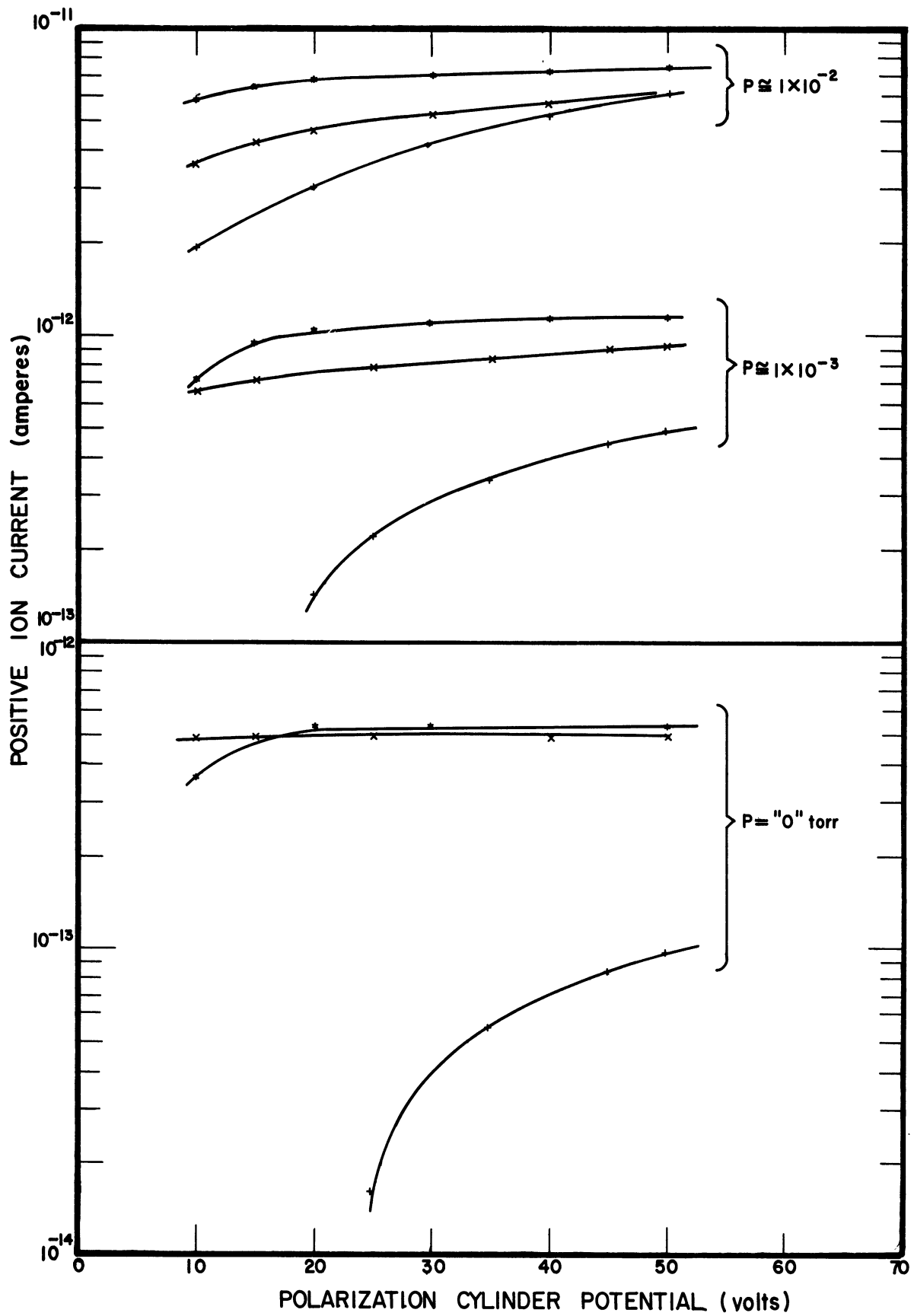
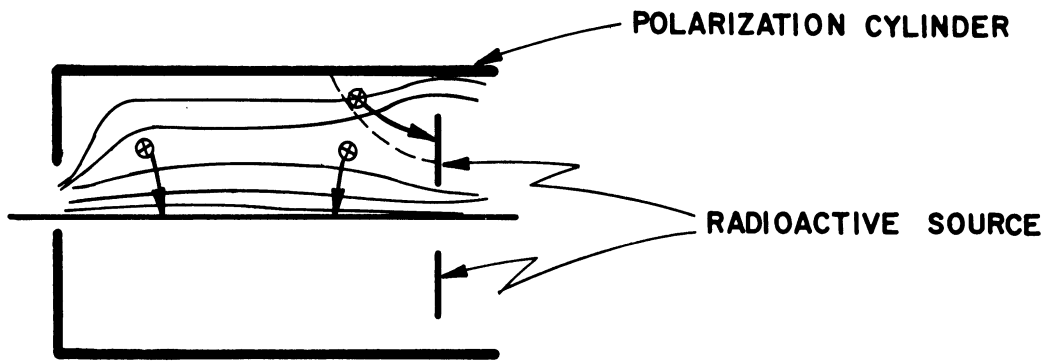
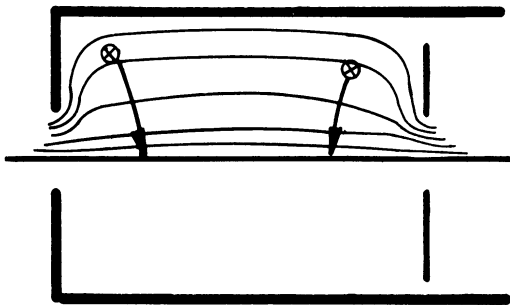


Figure 9. Cylindrical chamber characteristics, $P = 10^{-2}$, 10^{-3} , and "0" torr.



a) SOURCE POTENTIAL < CYLINDER POTENTIAL



b) SOURCE POTENTIAL = CYLINDER POTENTIAL



c) SOURCE POTENTIAL > CYLINDER POTENTIAL

Figure 10. Potential distribution within the ionization chamber.

In the design of a radioactive ionization gauge, one of the simplest possible configurations for construction would be to design the gauge so that the radioactive source will be electrically at ground potential. If this design had been used, a more detrimental effect would have been observed in addition to the collected ion boundary effect described above. With the ion collector at ground potential bias in order to minimize stray current leakages, electrons liberated by the passage of alpha particles through the sealing overcoat of the source would be able to strike the ion collector. The current measurement would then be the sum of the positive ion current and this electron (negative) current. The effect of this electron current is easily seen in Figure 9 for the condition when the source was maintained at 0 V. At the higher pressure levels, this effect is greatly reduced because of the shielding afforded by the neutral gas particles. However, at low pressures the effect of this electron current is quite pronounced. For the configuration mentioned, at a given operating potential the ion current-pressure linearity would be very poor. Of greater importance, however, is the fact that the energy of these electrons is less than about 20 eV and, of course, that the electrons have little mass. As a result, the electron current would be sensitive to such things as surface contaminants, temperature changes, and collector bias changes. These factors are believed to be the causes of the erratic and nonrepeatable current measurements observed at low pressures for this particular design.

In summary, the conditions at the ends of the cylindrical ionization chamber have an important effect on the ion current output. By maintaining the ends of the chamber at the same potential as the outer cylinder, flat, stable current characteristics are obtained. In addition, by applying a potential to the source, which in this design is one end of the ionization chamber, electrons liberated from the source are not able to strike the ion collector. As a result, stable characteristics are obtained even at the low pressures.

6.1.2. Ion Current Characteristics

A more complete mapping of the ion current characteristics for the source and cylinder maintained at the same operating potential is shown in Figure 11. In general, the curves exhibit flat saturated current characteristics over a wide range of both pressure and operating potential. However, there are a number of regions encountered in the characteristics which produce a collected ion current that is nonlinear with pressure for a given operating potential.

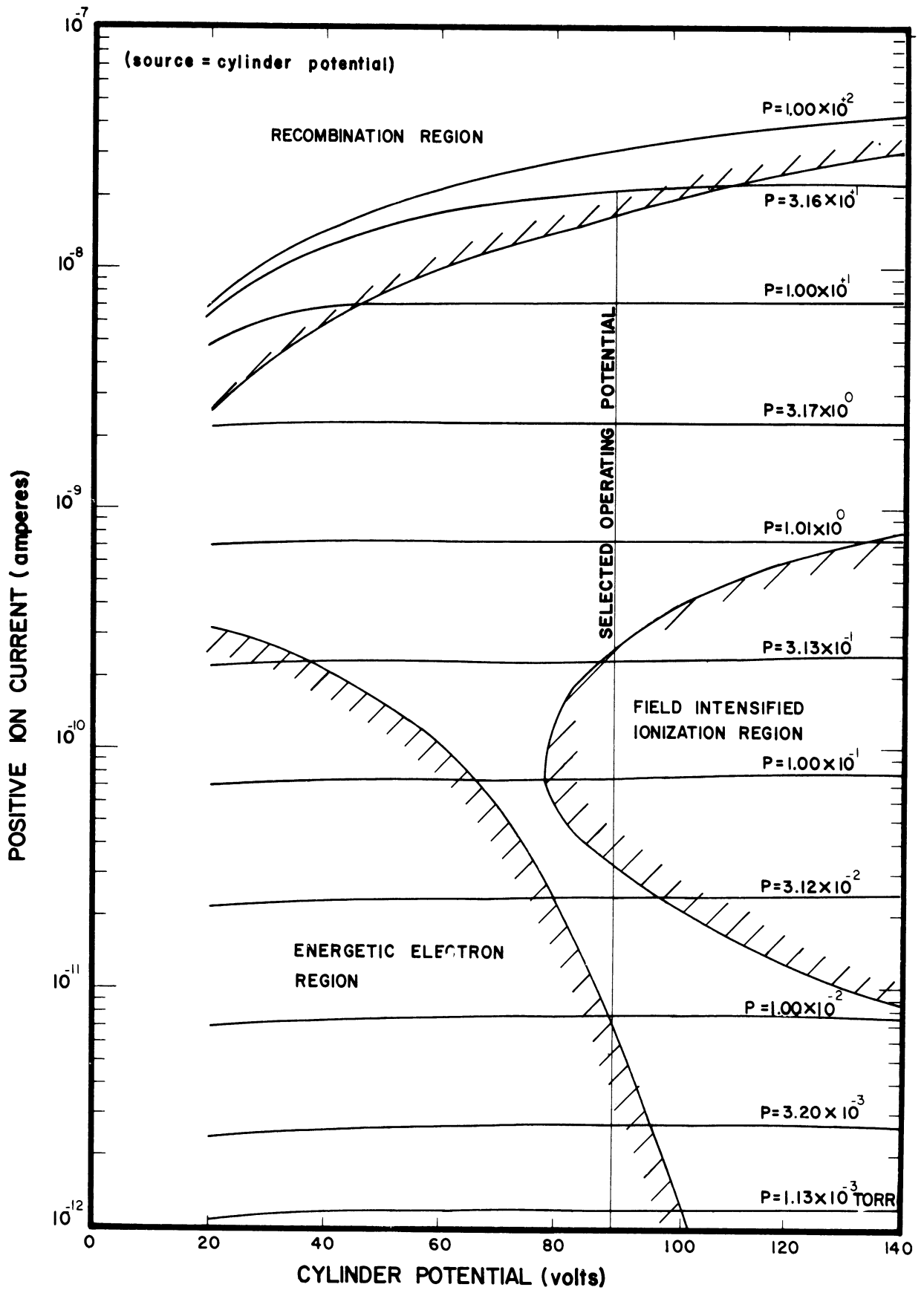


Figure 11. Summary, cylindrical chamber characteristics.

One of these regions is the recombination region. As can be seen, the nonlinear effect occurs predominantly at higher pressures. The effect is the result of electrons which have just been released in the ionization process becoming attached, yielding negative molecular ions. These negative ions and the positive ions which were also created in the ionization process are attracted to one another and may neutralize their charges to become neutral particles. This will have the result of reducing the ion current measurement to less than the expected saturated current level. Much of El-Moslimany's reported work (1960) dealt with the recombination region.

Another region encountered is at lower pressures and is the field-intensified ionization region. At the lower pressures, the probability of electron attachment is decreased and the free electrons are accelerated by the force caused by the electric field. When the kinetic energy gained by such electrons becomes high enough to ionize the gas molecules, an increase in the ionization occurs in addition to that due to irradiation by the alpha particles. This effect is the well known gas amplification phenomenon and can be circumvented by maintaining low operating potentials.

At the lowest operable pressures another effect is observed, noted in Figure 11 as the energetic electron region. This effect is believed to be due to electrons released in the gas ionization process having sufficient energy to enable a fraction of these to strike the ion collector. This has the result of reducing the ion current measurements to less than the expected saturated current level. At the higher pressures this effect shows a relative reduction due to the shielding provided by the increased neutral gas density. As could be expected, higher operating potentials also have the result of reducing the energetic electron effect.

The energetic electron effect was investigated in somewhat more detail in the 10^{-3} torr pressure region. At these pressures the neutral gas shielding mentioned above is minimal. The results are shown in Figure 12. The linear relation of ion current to pressure is also shown. S_1 is the sensitivity of the gauge determined in the 3 to 5 torr pressure range and I_R is the observed residual current at "zero" pressure.

As can be seen in Figure 12, the linear relation is more closely followed at the higher operating potential. This result, with the residual current observed to be insensitive to the operating potential, lends much support to the belief that the energetic electrons are created from the gas ionization process and that the electrons are not, for example, ejected from the walls of the chamber because of irradiation by the alpha particles.

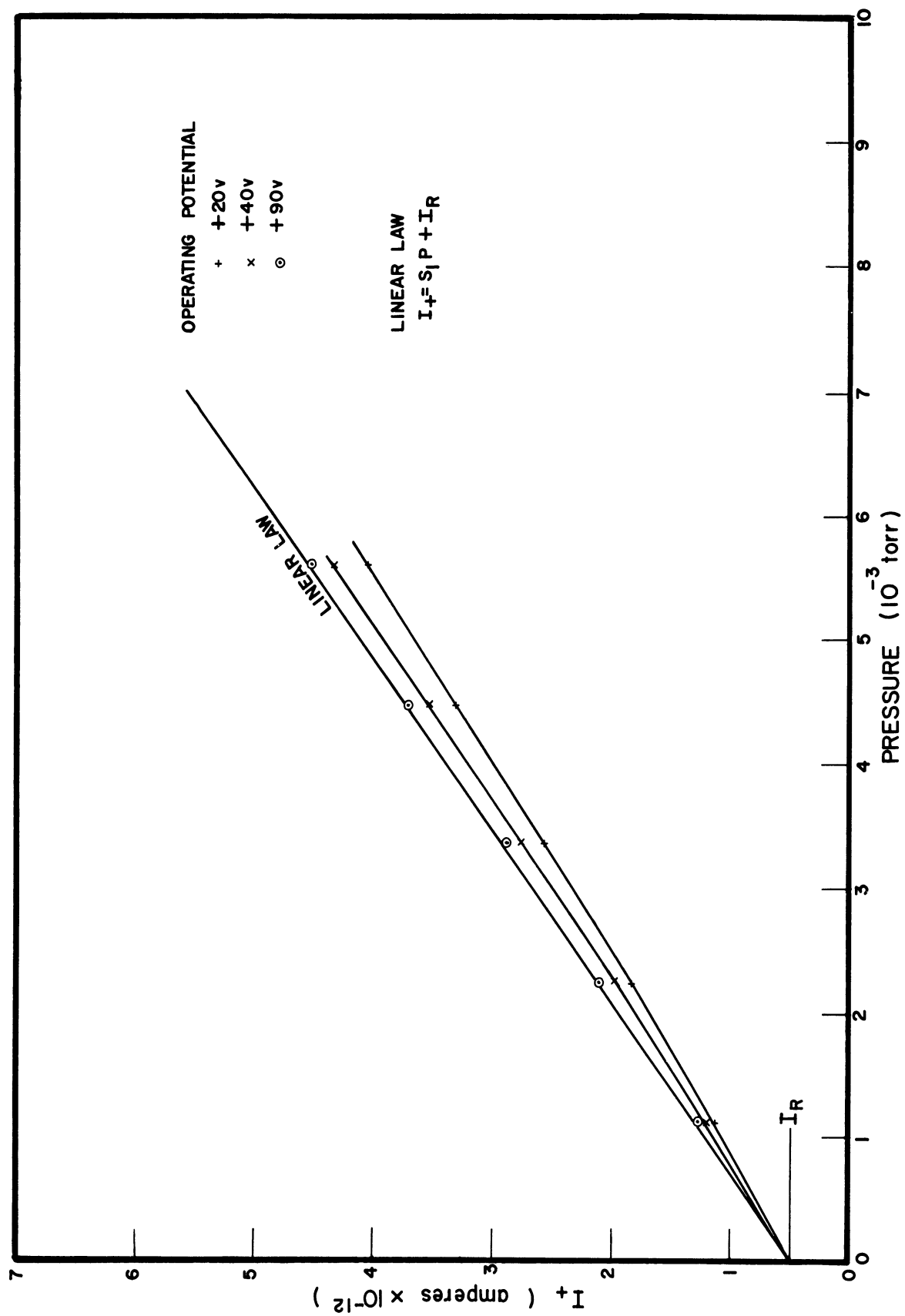


Figure 12. Effect of polarization potential (energetic electron region).

6.1.3. Residual Current at "Zero" Pressure

Also characteristic of these gauges is the relatively high residual current existing at "zero" pressure. The residual current is shown in Figure 13 to be dependent on the amount of source activity as well as on the collector surface area. The residual current is due to electrons being ejected from the ion collector and in effect appears to be the same as a positive ion current.

Various theories have been proposed to explain the mechanism causing this current. Two of the more plausible theories are these:

- (1) Soft X-rays, emitted from the walls of the chamber because of irradiation by the alpha particles, strike the ion collector and eject electrons;
- (2) electrons are ejected from the ion collector because of direct alpha particle bombardment.

The results of some laboratory testing using different collector materials favor the theory of direct bombardment by alpha particles. However, these results are not conclusive. A thorough investigation has not been undertaken to determine the exact nature of the mechanism causing the residual current. An effort directed at reducing the residual current so that lower pressure measurements could be made is not warranted at the present time because of the practical limitations imposed by the difficulties encountered with the signal conditioning of these low currents.

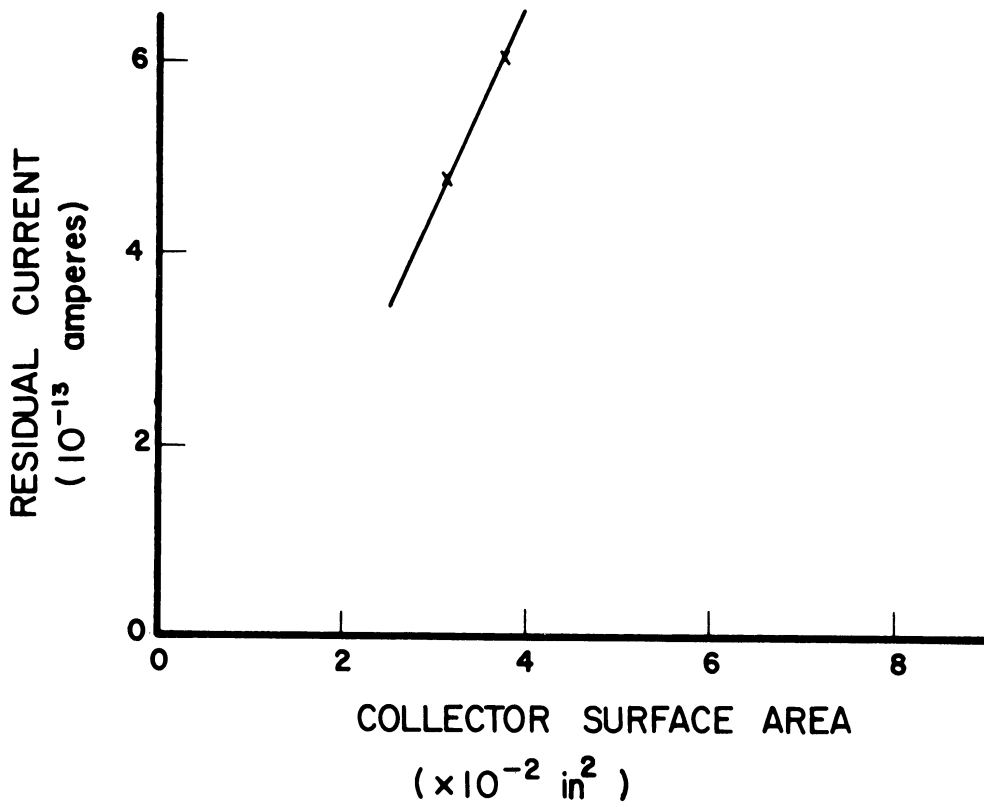
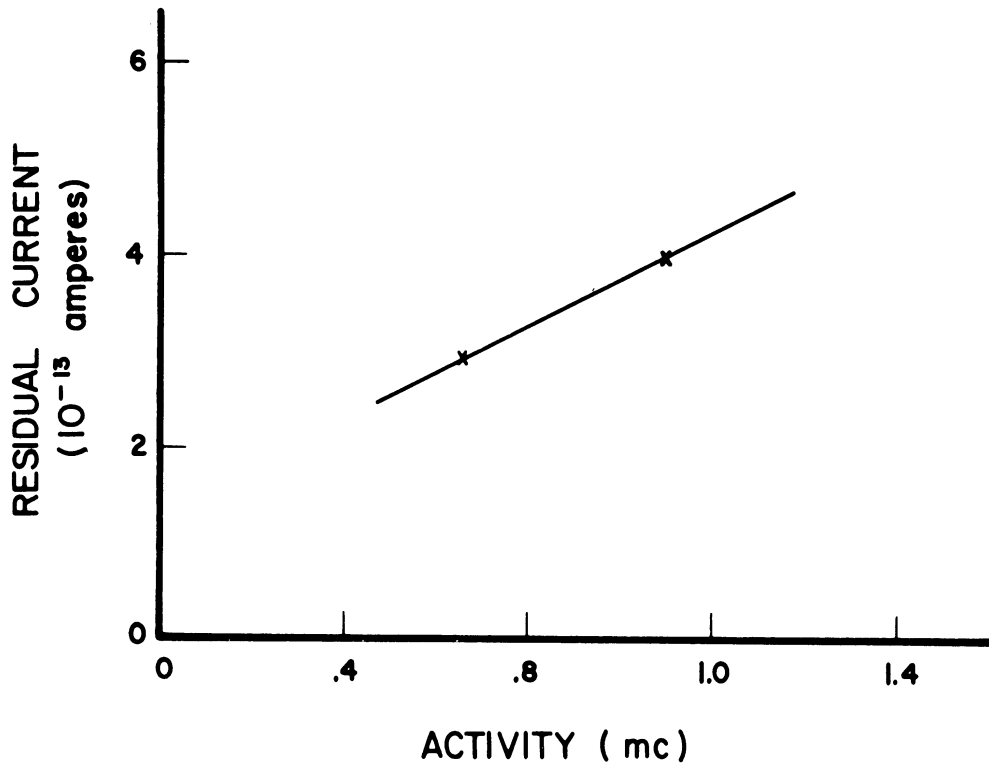


Figure 13. Residual current vs. source activity and vs. collector surface area.

6.2. PLANAR IONIZATION CHAMBER

6.2.1. Chamber Design

As can be seen in Figure 11, the recombination effects limit the cylindrical ionization chamber to measurements below approximately 20 torr. The design objective for the radioactive ionization gauge, however, was to be able to measure pressures to 1000 torr, so a planar ionization chamber was designed to measure pressures from approximately 10 to 1000 torr. The planar configuration was chosen because of the geometries involved and because of the greater electric field strengths and shorter ion travel distances to the ion collector that are needed in order to retard the recombination effects at these higher pressures.

The planar configuration is constructed by utilizing the source as one of the boundaries of the chamber, and by using a stainless steel screen, attached to the same feedthrough pins that the source is mounted on, as the other electrical boundary. A second stainless steel screen serving as the ion collector is immersed between the two boundaries as shown in Figure 14.

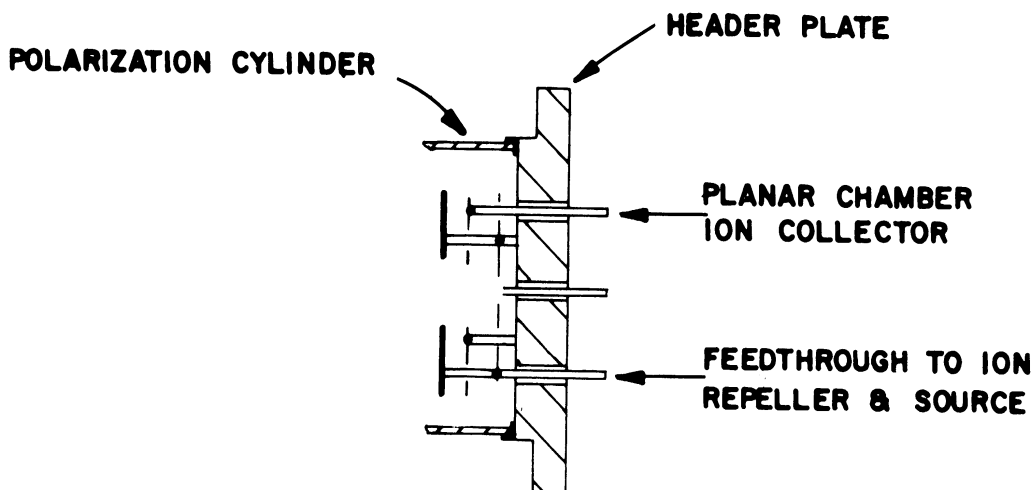
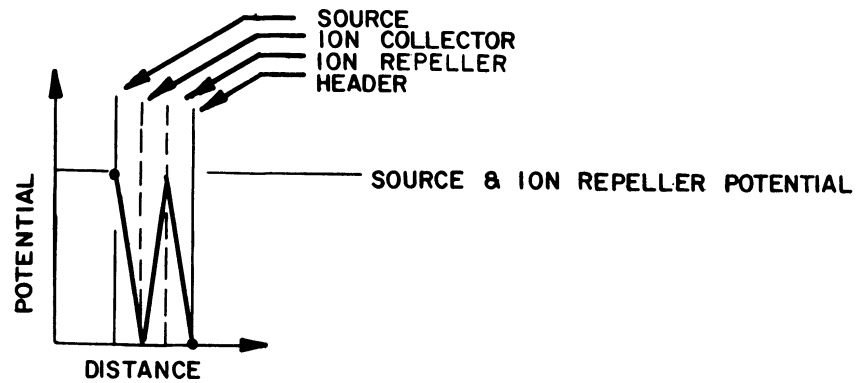
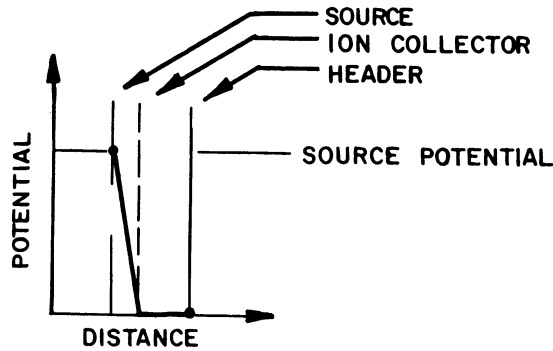


Figure 14. Planar chamber configuration.

A sketch of the potential variation between the source and screen is shown in Figure 15. The use of an ion repeller eliminates a neutral region between the ion collector and the header which would have existed if the ion repeller had not been used. Associated with the neutral region have been hysteresis and repeatability problems. The use of an ion repeller eliminates these problems and produces relatively strong field strengths throughout the major portion of the ionization chamber.



**a) PLANAR CHAMBER POTENTIAL VARIATION
(WITH ION REPELLER)**



**b) PLANAR CHAMBER POTENTIAL VARIATION
(WITHOUT ION REPELLER)**

Figure 15. Potential variation with and without ion repeller.

6.2.2. Effects of Various Cylinder Potentials

Positive ion currents measured as a function of plate potential show the effect of different potentials applied to the cylinder for three different pressures (Figure 16). As can be seen from these results, the conditions imposed around the outer diameter of this planar chamber greatly affect the ion current measurements. Similar to the various configurations involving the cylindrical chamber, a collected ion boundary also exists around the outer portion of this chamber. The position or location of this collected ion boundary is, of course, determined by the potential applied to the cylinder for a given pressure and source potential.

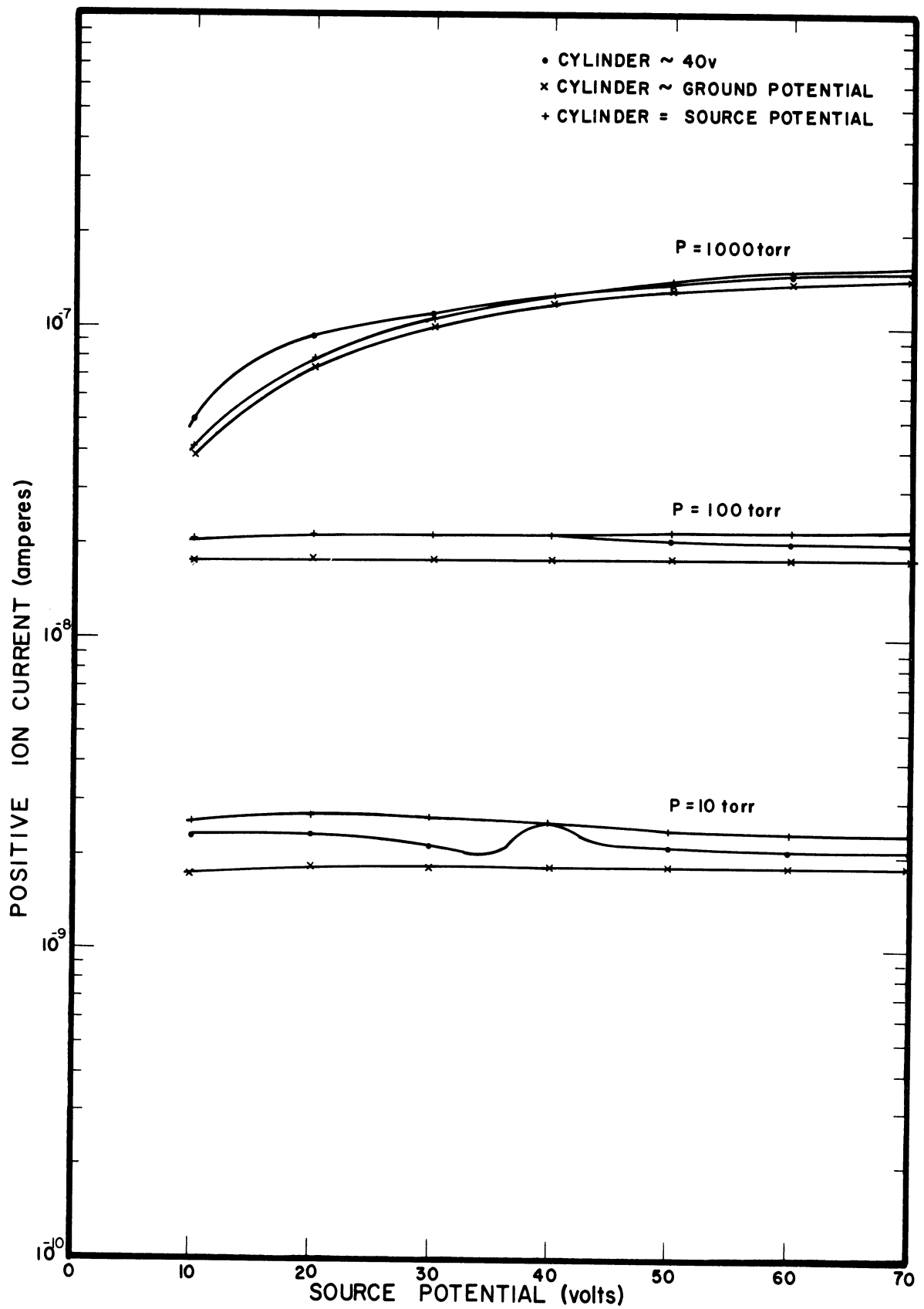
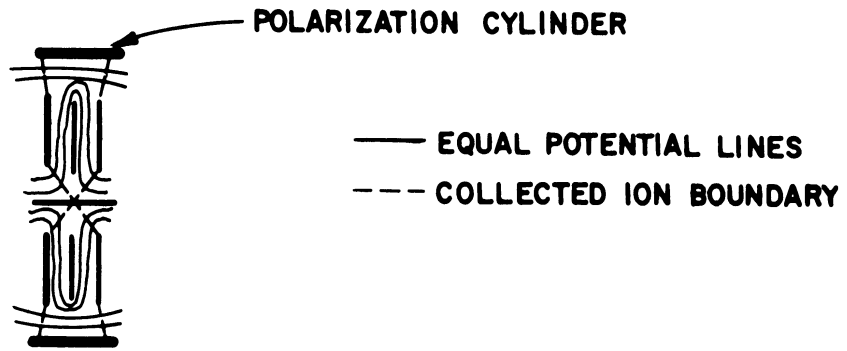


Figure 16. Planar chamber characteristics, P = 10, 100, and 1000 torr.

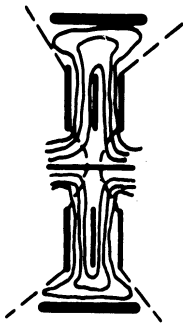
A sketch of the potential distribution and the approximate location of the collected ion boundary about the outer perimeter of this planar chamber is shown in Figure 17. At the high pressures, ion-ion recombination effects will completely dominate in any portion of the gauge which has weak electric fields or dead spots. At low pressures the effect of ion-ion recombination may be negligible, and consequently the location of the collected ion boundary may be significantly different for the two pressure regions.

The transitional ion-ion recombination effect is quite pronounced when the polarization cylinder and the radioactive source are operated at the same positive potential. The effect can be observed in the results shown in Figure 16 as a distinct bump occurring in the current characteristics at a pressure of 10 torr but not at 100 torr. Actually, the change occurred rapidly between 20 and 30 torr, causing severe nonlinearity and loss of stability in this pressure range.

Operating the planar chamber with the cylinder at a higher potential than the source considerably improves the situation described above. However, the electrical configuration found most satisfactory was to ground the polarization cylinder potentially. With the cylinder at ground potential, the collected ion boundary is pulled in much closer to the ion collector. Practically, the local recombination effects in the dead region between the ion collector and the cylinder are kept out of the ion collection region. Consequently, the current characteristics with the cylinder at ground potential are observed to be quite flat and stable, except at 1000 torr where recombination effects are significant throughout the entire chamber volume at low electric field strengths.



a) POLARIZATION CYLINDER POTENTIAL > SOURCE/ION REPELLER POTENTIAL



i LOW-PRESSURE



ii HI-PRESSURE (> 30 torr)

b) POLARIZATION CYLINDER POTENTIAL = SOURCE/ION REPELLER POTENTIAL



c) POLARIZATION CYLINDER POTENTIAL = 0 VOLTS

Figure 17. Planar chamber potential distribution.

6.2.3. Ion Current Characteristics (Planar Chamber)

A more complete mapping of the ion current measurements with the cylinder maintained at ground potential is shown in Figure 18. The ion-ion recombination region and the field intensified ionization region are both quite evident for the planar chamber. The energetic electron effects are completely masked at the higher pressures. Between the two pronounced regions, from pressures of approximately 10 torr to 1000 torr, stable, saturated current characteristics exist. This is the desired operating range and meets the design objective for this chamber.

An interesting effect is observed in the characteristics shown in Figure 18. The saturated current levels for the 1000 torr and 316 torr pressure values are slightly closer together than the spacing of the other saturated current levels just below these. This effect occurs only at high pressures and is due to the finite kinetic energy of an emitted alpha particle being expended in the ionization process in a relatively short pathlength. At a pressure of 1000 torr, the alpha particles emitted from the Americium-241 source have a mean range in air of approximately 1 in. or slightly less. This is of the order of the planar chamber dimensions. Consequently, those alpha particles which are stopped before they traverse completely across the chamber will produce essentially a constant number of ion pairs independent of pressure. The result of this is a loss of linearity at the higher pressures.

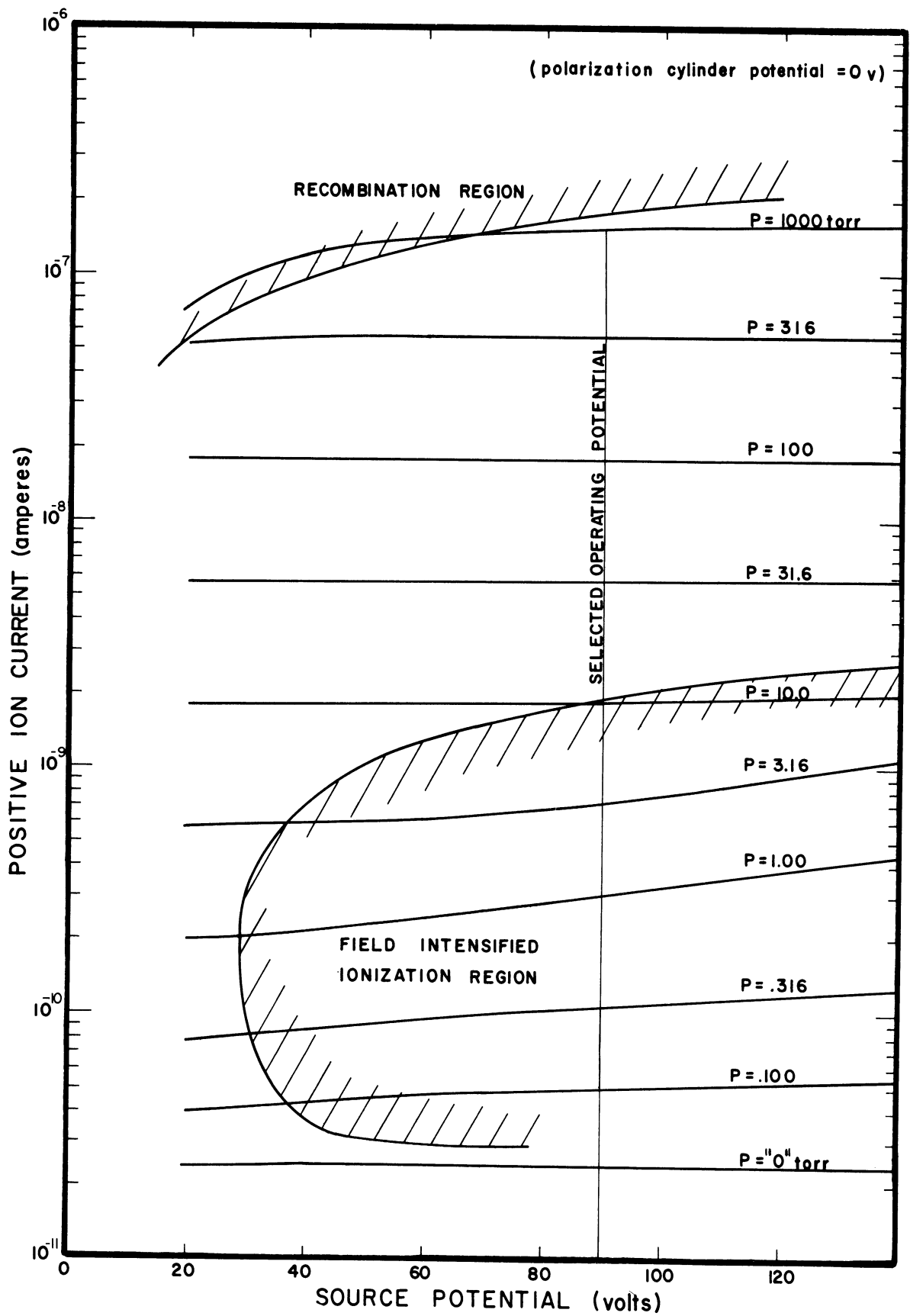


Figure 18. Summary, planar chamber characteristics.

7. GAUGE OPERATION

The collected positive ion current from the dual collector ionization gauge in its useful pressure measurement range of 10^{-3} torr to 1000 torr is shown in Figure 19. The sensitivity of the gauge in the planar ionization chamber operating region is approximately 1.75×10^{-10} amps/torr, while in the cylindrical ionization chamber operating region the sensitivity is 6.5×10^{-10} amps/torr. The ratio of these two sensitivities is essentially the ratio of the two ionization chamber volumes.

From a pressure of 1000 torr to 10 torr, the high pressure ion collector in the planar ionization chamber is used. The source-plates in this pressure range are maintained at a potential of +90 V and the polarization cylinder is maintained at ground potential. The low pressure ion collector which is not used in this pressure region is also maintained at ground potential.

At a pressure of 10 torr and below, the low pressure ion collector in the cylindrical ionization chamber is used. Both the source-plates and the polarization cylinder in this range of pressures are maintained at +90 V potential. The high pressure ion collector which was used above a pressure of 10 torr is now maintained at ground potential.

The operating potential of +90 V was chosen in order to achieve good linearity from both ionization chambers over the entire pressure measurement range. During operation, when the 10 torr pressure level is crossed, a change in the potential applied to the polarization cylinder of 90 V occurs and coincides with the collector change. Overall, the gauge has a pressure-measuring capability of approximately six orders of magnitude.

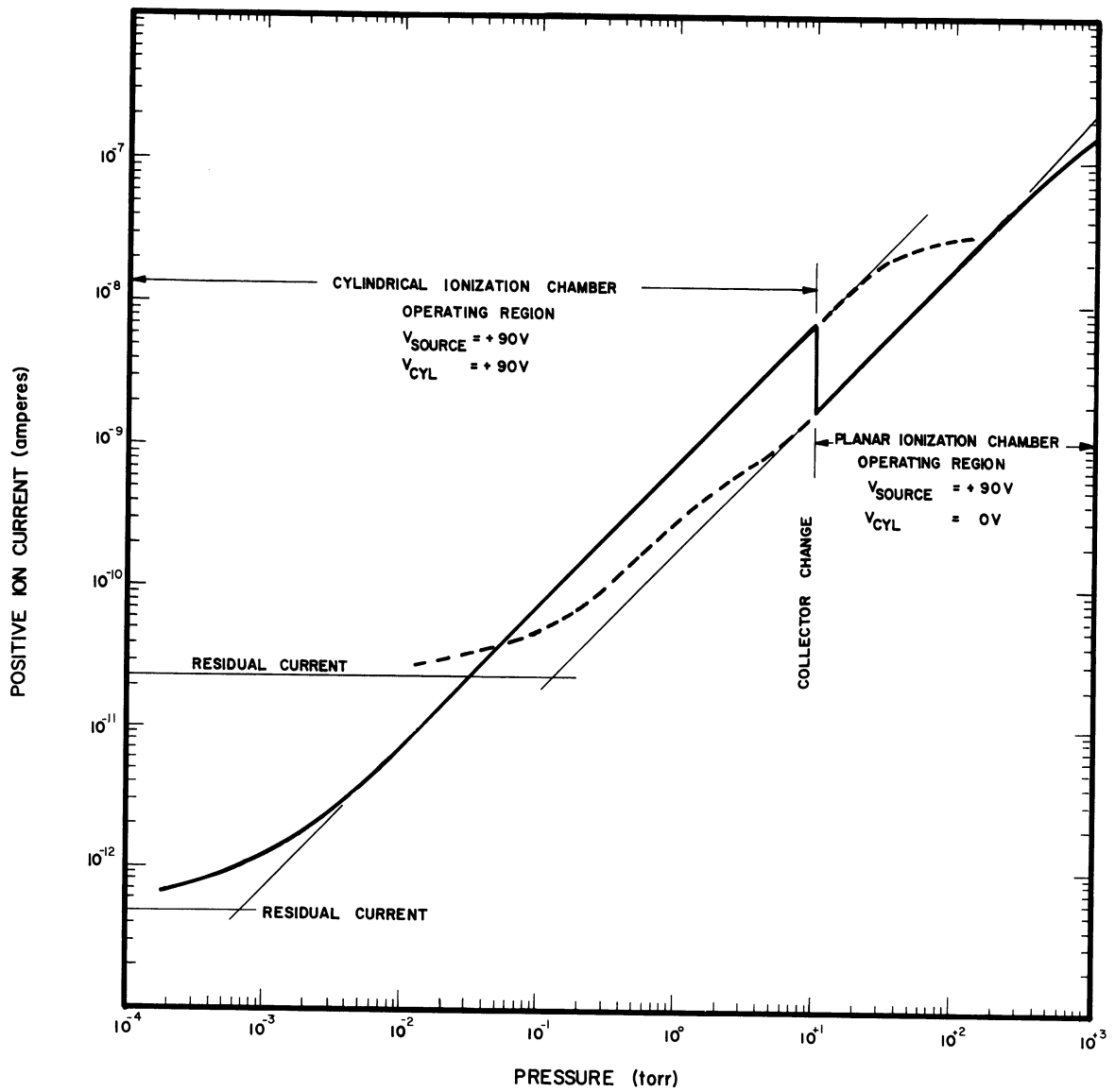


Figure 19. Dual collector gauge operating region, ion current vs. pressure.

8. GAUGE PERFORMANCE

8.1. LINEARITY

For general information the percent deviation of the ion current—pressure relationship from linear behavior for both the cylindrical chamber and the planar chamber is shown in Figure 20. The various regions, discussed previously and also shown in Figures 12 and 18, are clearly evident. For the cylindrical chamber operating range, zero percent deviation was established at a pressure of 4 torr, and for the planar chamber operating range, a pressure of 50 torr was chosen.

The operating potential of +90 V was selected to achieve good linearity with both chambers over the entire pressure range of 1×10^{-3} torr to atmospheric pressure. The percent deviation for an operating potential of +75 V is also shown and illustrates the relative insensitivity of the gauge to the operating potential.

To date, no concentrated effort has been made to improve the linearity of the gauge. To take into account the nonlinearity, a detailed calibration of each gauge is always performed.

8.2. LONG TERM STABILITY

Although gauge repeatability over relatively short time periods of a few days proved excellent, long term stability remained of some concern because in the present aeronomy program the gauges are calibrated approximately five weeks before their final use. Consequently, a calibration before and after a seven and one-half month time lapse was performed and was believed sufficient to detect any significant systematic change that might show up in the ion current.

The results of this test were somewhat as expected: less than $\pm 2\%$ changes were observed over the entire pressure measurement range of 1×10^{-3} torr to atmospheric pressure. The combined variations and changes due to the vacuum calibration system and in the electrometer amplifier used in the ion current measurements, even without considering any changes occurring within the radioactive ionization gauge, were anticipated to be of the order of the observed $\pm 2\%$ over this time period. Long term stability is consequently recognized as being one of the several merits of the gauge.

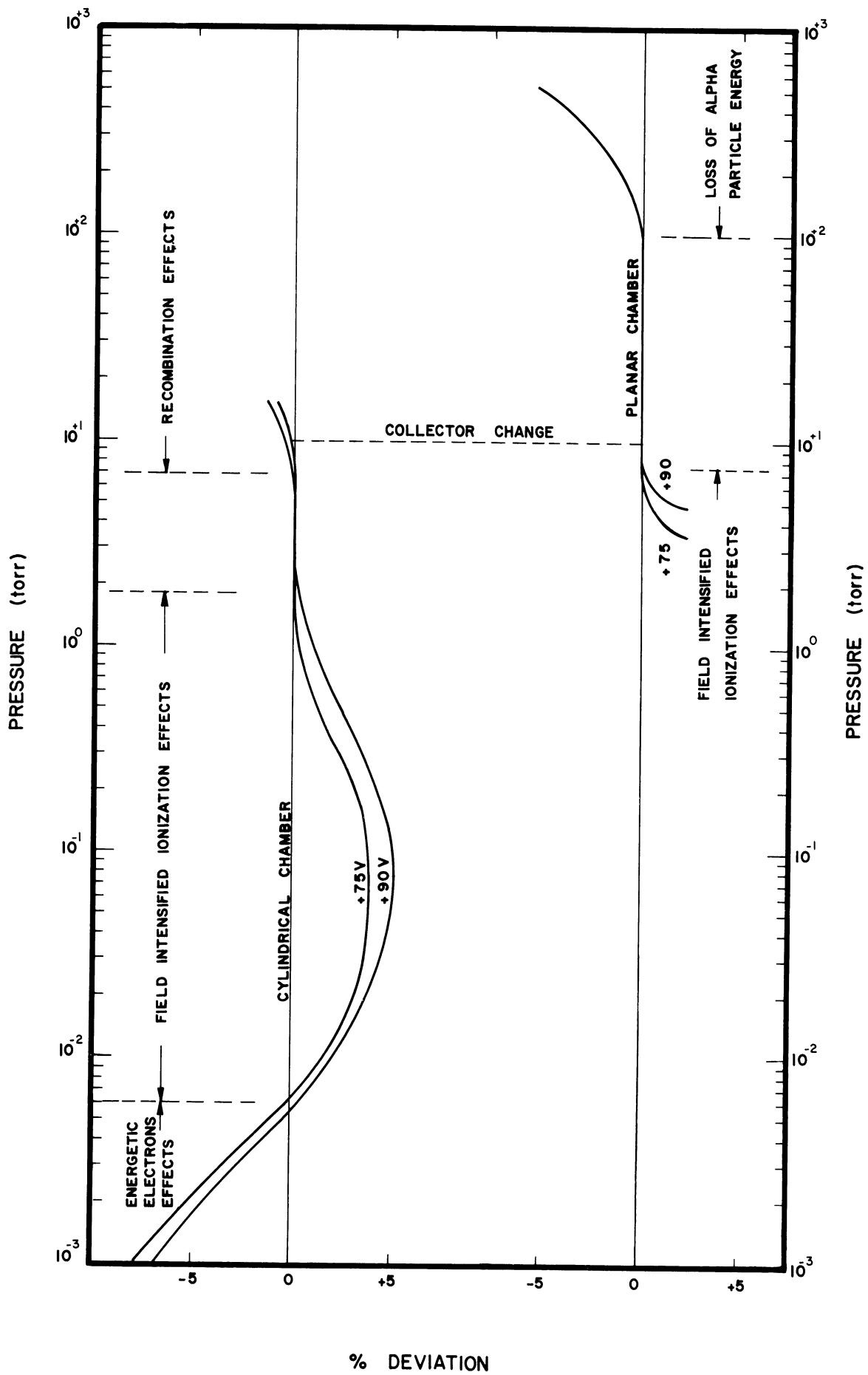


Figure 20. Gauge nonlinearity, both chambers.

8.3. TEMPERATURE EFFECTS

As one would expect, the radioactive ionization gauge is sensitive primarily to gas density. However, over a wide range of operating conditions, temperature effects might have been significant. Consequently, tests were conducted to determine the importance of these effects by operating the gauge at constant density and varying only its temperature.

A simple experiment was set up for these tests and is shown in schematic form in Figure 21. Ion current measurements were subsequently recorded in both increasing and decreasing temperature directions to eliminate possible errors due to temperature lag and to insure the absence of outgassing effects.

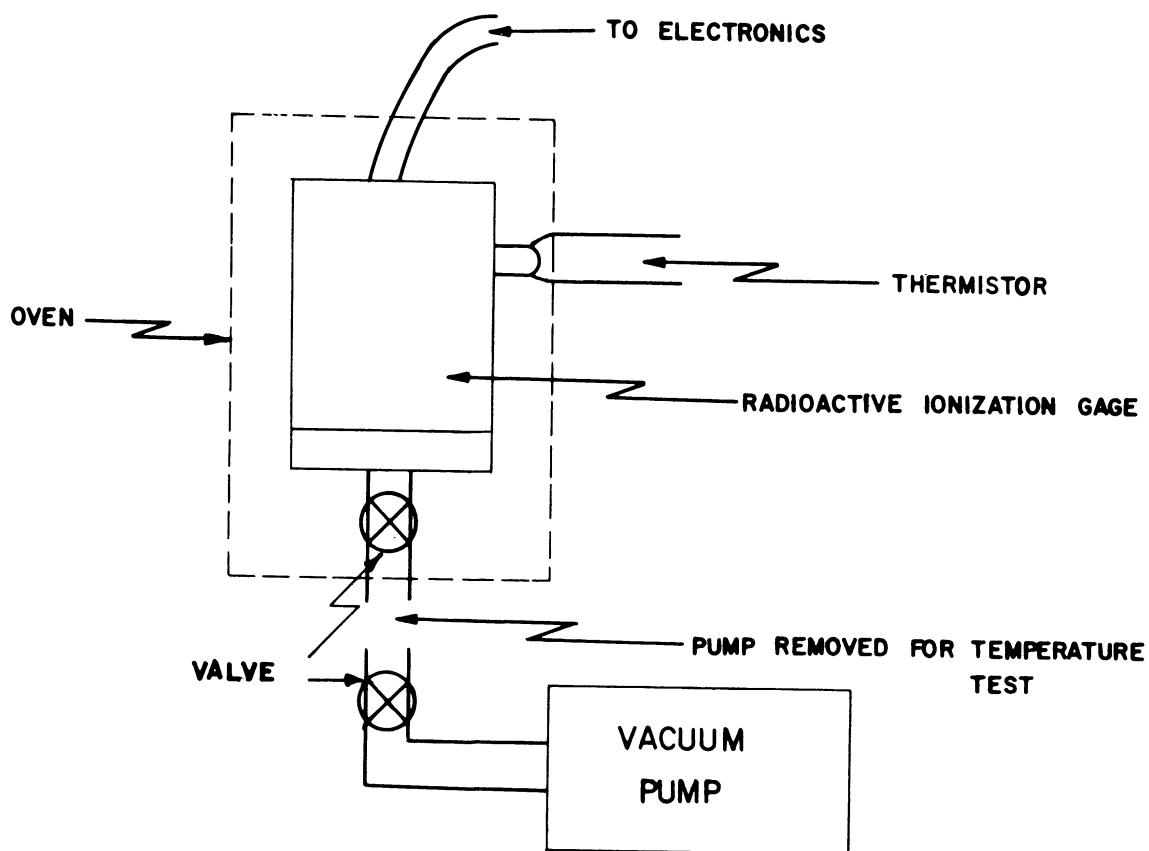


Figure 21. Temperature test setup.

Typical results of these tests conducted at constant gas density are shown in Figure 22, and illustrate the relative insensitivity of the gauge to temperature changes. The ion current variation is only approximately $+0.02\%/^{\circ}\text{C}$, also indicating a slight enhancement of the gas ionization process for increased temperatures. Of passing interest was the residual current, described earlier, which remained completely unchanged with increased temperatures.

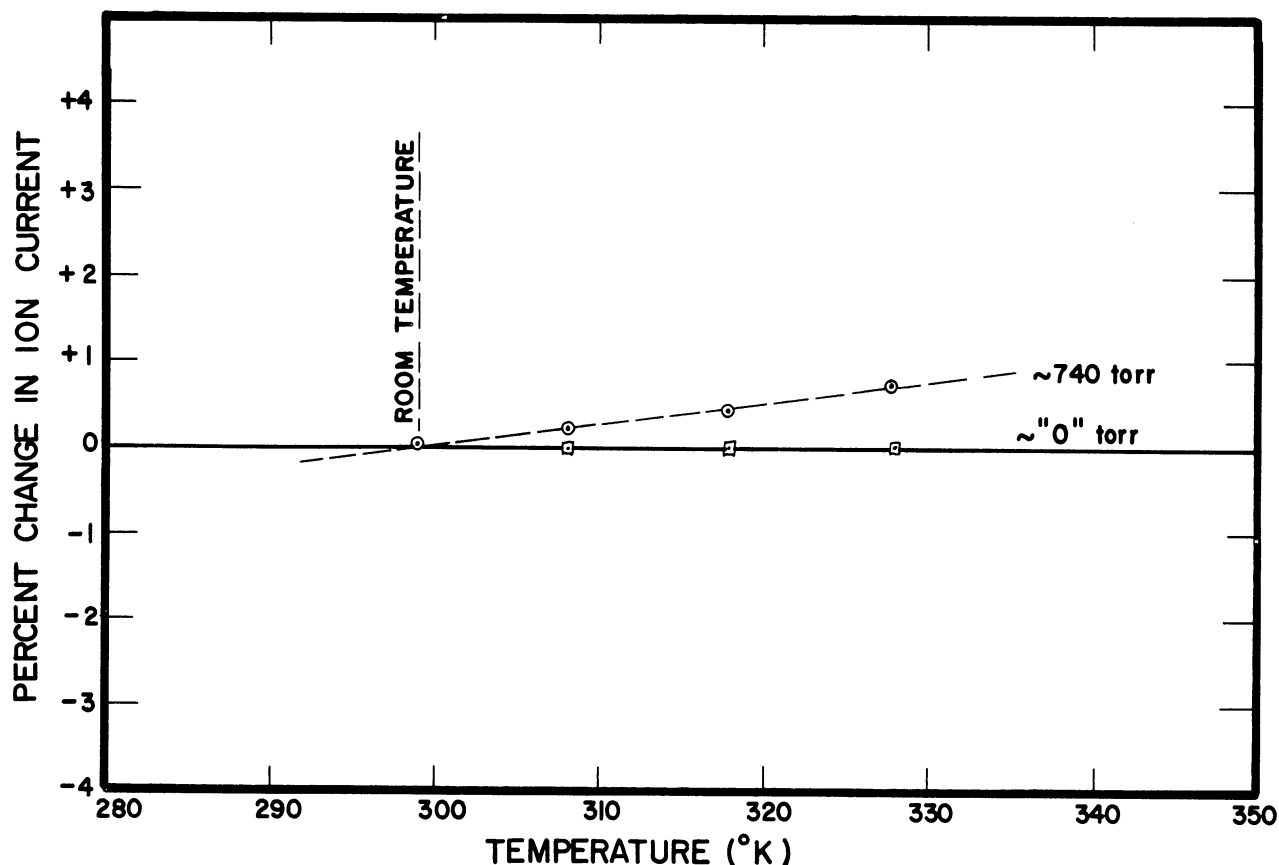


Figure 22. Percent ion current change vs. temperature for constant gas density.

8.4. HYSTERESIS

At the relatively high pressures over which the radioactive ionization gauge effectively operates, a change in vacuum system pressure is accompanied by a drop or rise in gas temperature due to the gas expansion or compression. Simultaneously, heat transfer tends to restore the gas temperature to the temperature of the confining walls. As a result, the absolute pressure as well as the time rate of change in pressure are determining factors in the gas temperature during a change in vacuum system pressure.

The variation in gas temperature was observed indirectly when pressure cycling with the vacuum system was performed. An apparent hysteresis was noted during the pressure cycling if the measurements from the radioactive ionization gauge, which is a gas density sensor, were interpreted directly as pressure measurements. However, this effect is the result of considering pressure and density synonymous, which, of course, is invalid if the gas temperature does not remain constant. The magnitude of the effect was found to depend not only on the time rate of change in pressure, but also on the decade of pressure in which the changes were performed. At lower pressures, the ef-

fect became vanishingly small as the result of longer mean free paths and more rapid accommodation of the gas to the wall temperature. Hence, for pressure measurements with a radioactive ionization gauge, knowledge of the gas temperature is mandatory.

9. CONCLUSIONS

In the design of the radioactive ionization gauge for upper atmosphere measurements several objectives were pursued. A simple, rugged construction for use on sounding rockets was conceived and has since proved reliable. For the ionizing source in the gauge, Americium-241 impregnated foil, nominally of 7 mc activity, was found quite acceptable although the gauge sensitivity is an order of magnitude lower than what would be considered ideal.

Flat, stable operating characteristics were one of the major objectives in the design of the gauge and for these, the electrical configuration proved most important. For measurements over the wide dynamic range of 1000 to 10^{-3} torr, two ion collectors were necessarily employed. In general, the performance of this gauge has been quite satisfactory.

10. REFERENCES

- Ainsworth, J. E., D. F. Fox, and H. E. LaGow, "Upper Atmosphere Structure Measurement Made with the Pitot-Static Tube," Journal of Geophysical Research, 66, No. 10, pp. 3191-3212, 1961.
- Downing, J. R. and Glenn Mellen, "A Sensitive Vacuum Gauge with Linear Response," The Review of Scientific Instruments, 17, No. 6, June 1946.
- El-Moslimany, M. A., Theoretical and Experimental Investigation of Radioactive Ionization Gauges, University of Michigan Scientific Report 03554-4-S, May 1960.
- Flanick, A. P. and J. E. Ainsworth, "Vacuum Gauge Calibration System (10^{-2} to 10^1 mmHg)," The Review of Scientific Instruments, 32, No. 4, pp. 408-410, April 1961.
- Horvath, J. J., R. W. Simmons, and L. H. Brace, Theory and Implementation of the Pitot-Static Technique for Upper Atmosphere Measurements, University of Michigan Scientific Report 04673-1-S, March 1962.
- Liverhant, S., Elementary Introduction to Nuclear Reactor Physics, John Wiley and Sons, New York, 1960.
- Simmons, R. W., An Introduction to the Theory and Data Reduction Method for the Pitot-Static Technique of Upper Atmosphere Measurement, University of Michigan Scientific Report 05776-1-S, March 1964.
- Spencer, N. W., R. L. Boggess, L. H. Brace, and M. A. El-Moslimany, A Radioactive-Ionization-Gage Pressure-Measurement System, University of Michigan Scientific Report ES-1, 2597-3-S, May 1958.
- Strain, J. E. and G. W. Leddicottee, The Preparation, Properties, and Uses of Americium-241, Alpha-, Gamma-, and Neutron Sources, Analytical Chemistry Division, Oak Ridge National Laboratory, Oak Ridge, Tennessee, September 1962.
- Vacca, R. H., "Recent Advances in the 'Alphatron' Vacuum Gauge," 1956 National Symposium on Vacuum Technology Transactions, Edmond S. Perry and John H. Durant, editors, Pergamon Press, New York, pp. 93-100.
- Zito, George V., Appendix D: Radioactive Ionization Air Density Sensors: The State of the Art 1959, Fifth Monthly Progress Report submitted to Wright Air Development Center by Litton Industries Electronic Equipment Division, Beverly Hills, California, December 1959.

APPENDIX A

ION CURRENT DETECTOR

For the measurement of the small ion currents, a multirange electrometer amplifier was used. A detailed description of this amplifier, which was developed, built, and flown by this laboratory, will not be presented here since a report on the instrument is in preparation elsewhere. However, a brief explanation will be given. A block diagram of the amplifier is shown in Figure 23. The current to be measured is, in effect, passed through a high-meg resistor, and the voltage drop appears as a portion of the voltage in the feedback loop of the amplifier stage, for which β , the feedback factor, is near unity. Thus, a voltage change at the output of the amplifier is nearly equivalent in magnitude to the voltage change across the high-meg resistor but opposite in sense.

The ion currents, as shown in Figure 19, vary over more than five orders of magnitude. For measurements over this range of ion current five high-meg resistors are employed. These resistors are changed or switched by glass encapsulated reed relay switches utilizing fully automatic range switching circuitry. A ratio of 16 for the high-meg resistor ranges was chosen except where collector switching occurs. The upper switch point of -20.0 V and the lower switch point of -1.10 V were selected to provide switch point hysteresis and minimize the possibility of switching chatter when a range change occurs.

The normal output of 0 to -20 V from the electrometer amplifier is then inverted in sign and sub-ranged by an inverter amplifier, providing an output of 0 to +5 V which is compatible with existing telemetry systems. For the sub-ranging, gains of 1.0 and 0.25 were selected for the two-gain state inverter amplifier. A Schmitt trigger is used which senses the electrometer amplifier output and provides the control of a solid state switch that determines the feedback impedance and consequently the gain of the inverter amplifier. The set points of the Schmitt trigger are adjusted for -5 V and -4.4 V, again providing switch point hysteresis.

The scheme and sequence for the switching logic is shown in Figure 24. For the switching of the polarization cylinder potential and ion collectors, the existing logic employed for the fully automatic switching of high-meg resistor No. 4 was utilized. Again, glass encapsulated reed relay switches were used. The high-meg resistor values were selected so that switching of the polarization cylinder potential and ion collectors occurred simultaneously at a pressure of approximately 10 torr.

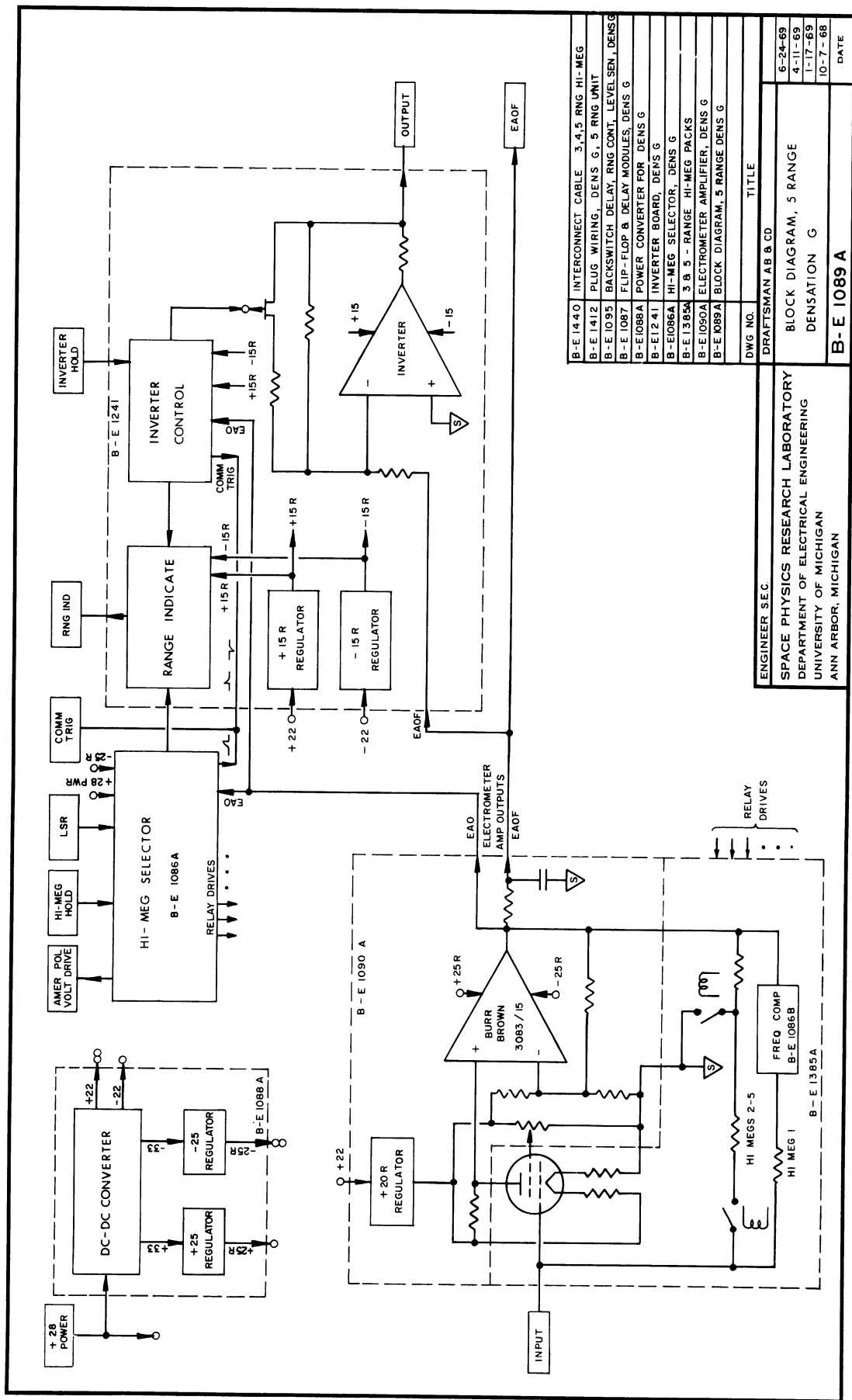


Figure 23. Electrometer amplifier block diagram.

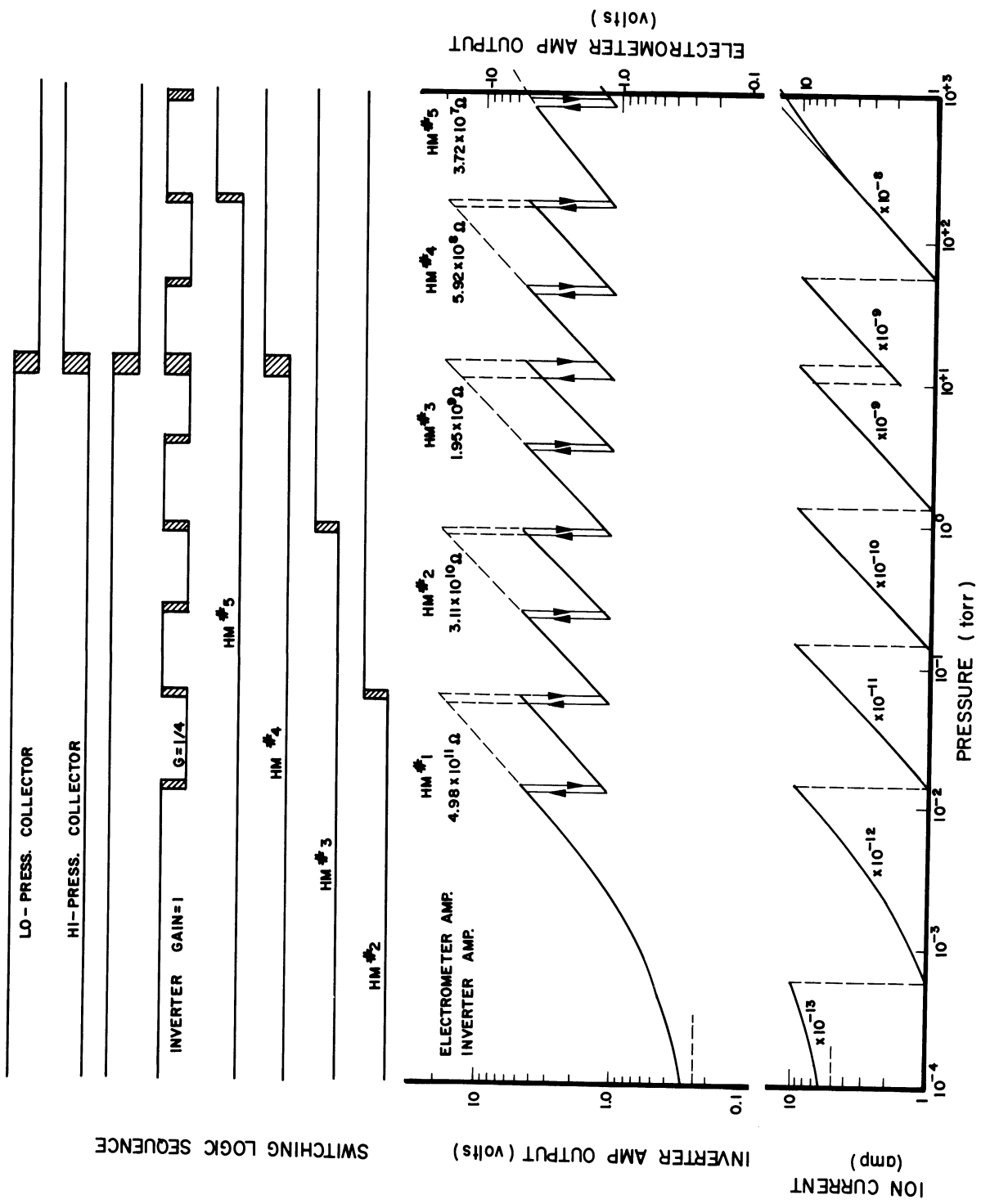


Figure 24. Electrometer amplifier switching sequence.

APPENDIX B

VACUUM SYSTEM

For the assembly, handling, and pressure calibration of the radioactive ionization gauges, a special facility was constructed. Part of this facility houses the monitoring equipment and the air ventilation system which are necessary in work with radioactive materials. For the purpose of calibrating the ionization gauges, a rather complete vacuum laboratory is enclosed by the other part.

The low vacuum (high pressure) calibration system used for the gauge investigation, fabricated over a period of time, is continually being modified and updated. The pump for this system is a turbo-molecular vacuum pump manufactured by the Welsh Scientific Company. One of the chief advantages of this pump is its relatively high pumping speed which is useful for dynamic pressure studies.

Figures 25 and 26 are views of the vacuum system. The prototype radioactive ionization gauge can be recognized on the top of the vacuum system at the left in Figure 25 and on the right in Figure 26. Part of a pitot probe rocket payload, mounted on the vacuum system for calibration, is at the right in Figure 25 and at the left in Figure 26. Views of the calibration control console and vacuum system control panel are shown in Figures 27 and 28.

Pressure measurements are obtained by employing the slug-input technique (Flanick and Ainsworth, 1961) in conjunction with the MKS capacitance manometer manufactured by the Baratron Corporation. This calibration system is believed capable of pressure measurements within an accuracy of $\pm 1\%$ absolute from atmospheric pressure to 10 torr, which do not exceed $\pm 4\%$ absolute at a pressure of 1×10^{-3} torr.

On a relative basis, from calibration to calibration, pressure measurement capability with the use of this vacuum system is believed to be within $\pm 1\%$ over the entire pressure range from atmospheric pressure to 1×10^{-3} torr. During the present gauge investigation ultradry air was used exclusively.

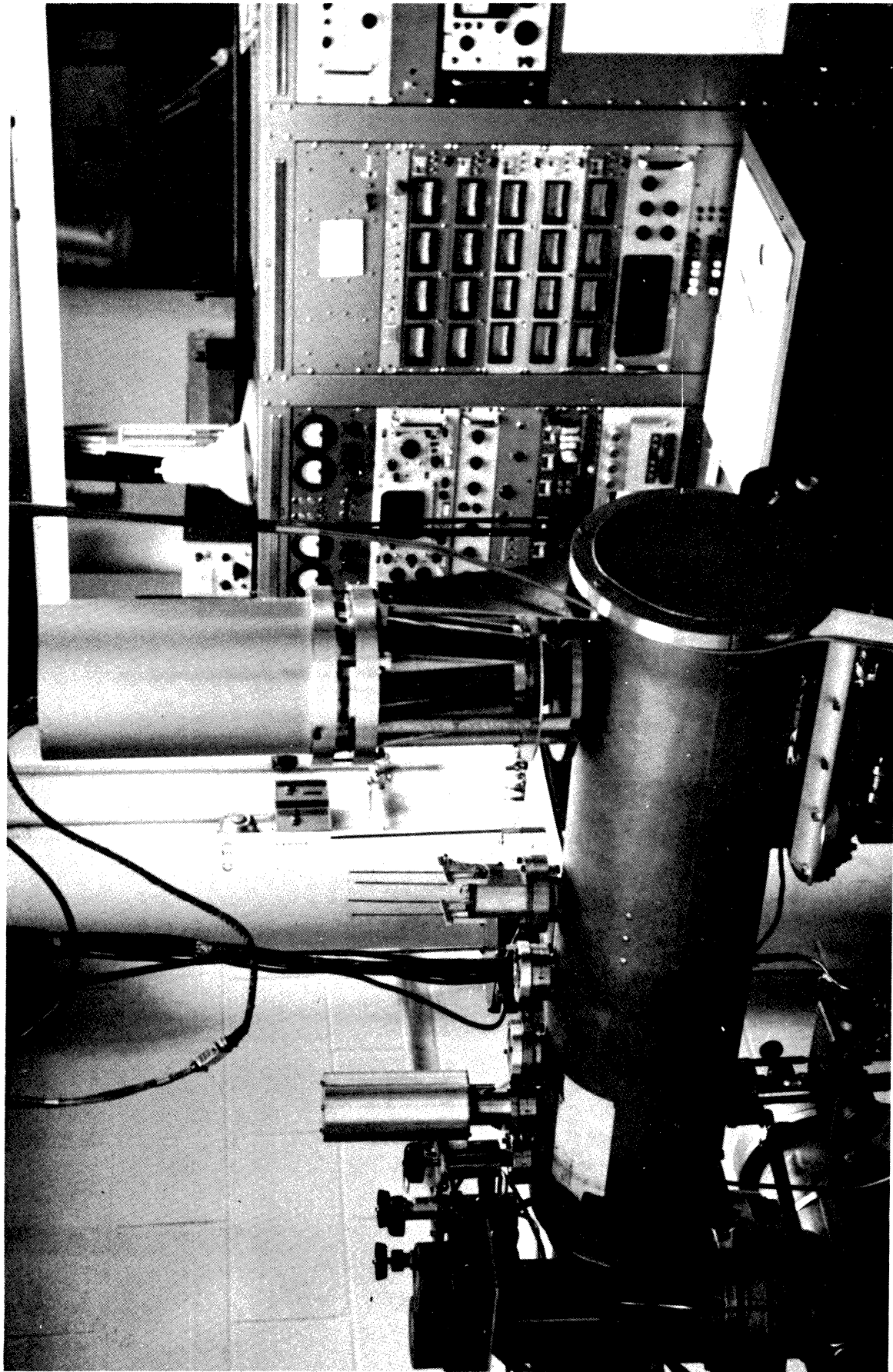


Figure 25. Vacuum system and calibration control console.

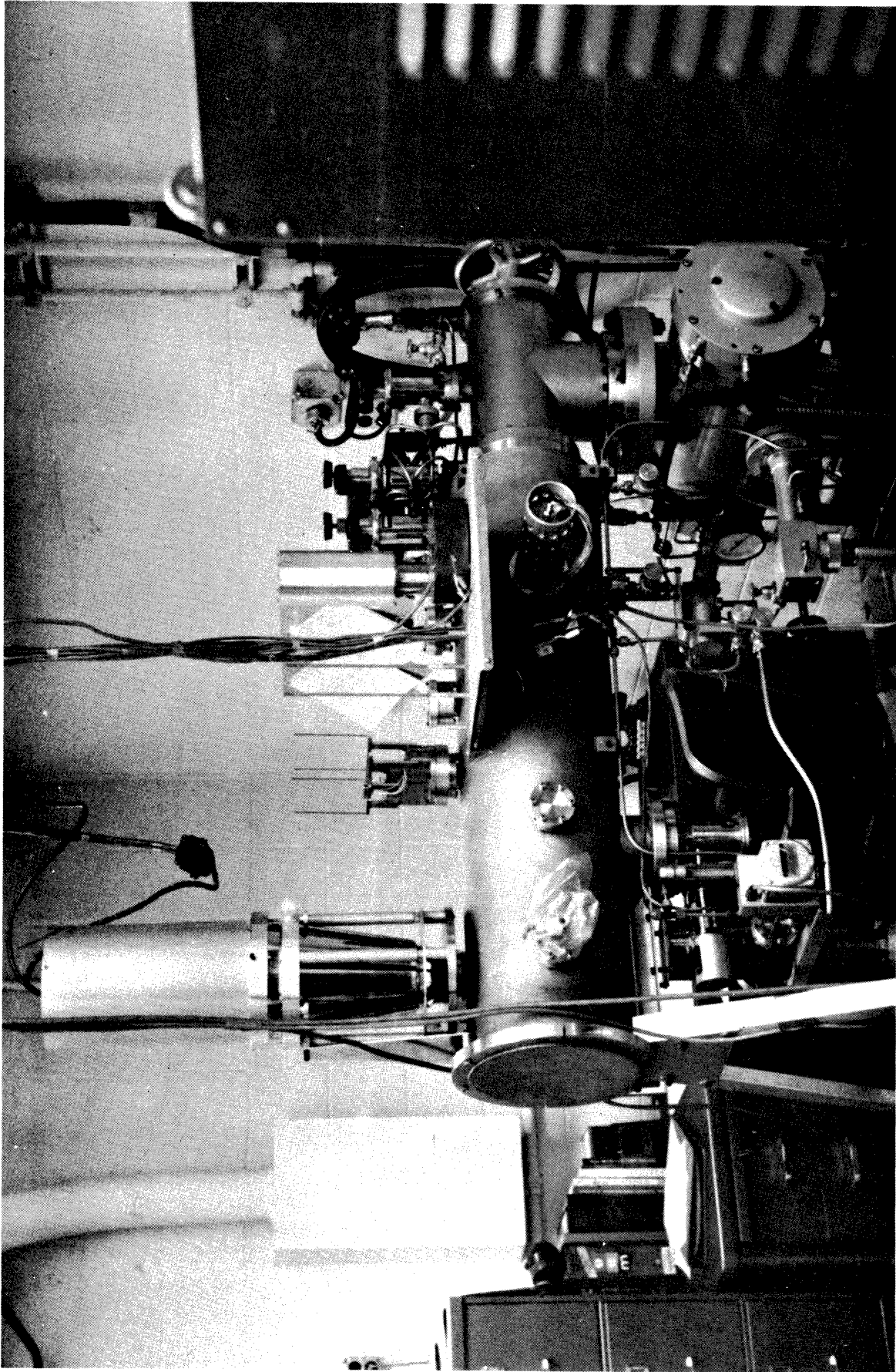


Figure 26. Vacuum system.

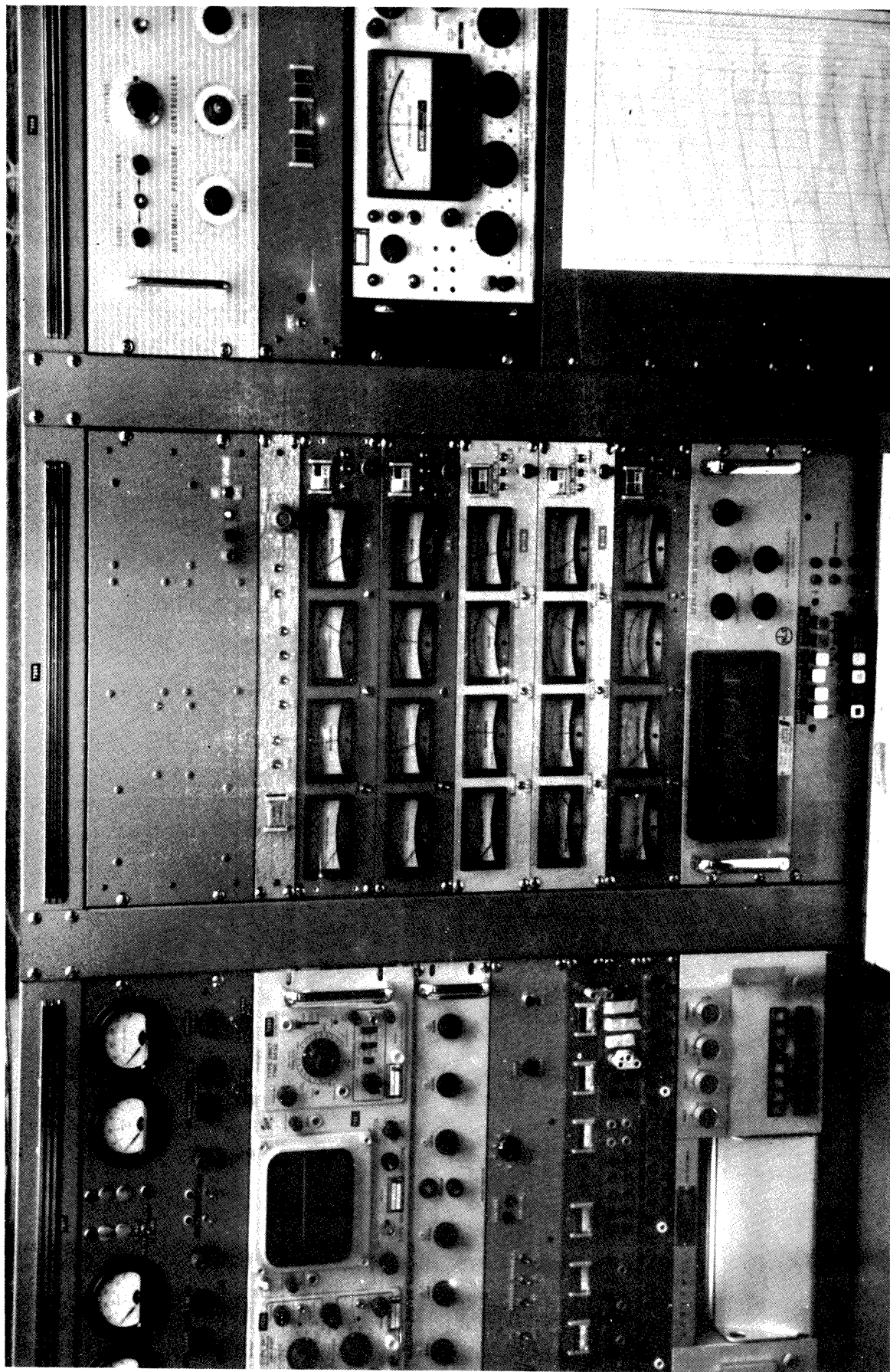


Figure 27. Calibration control console.

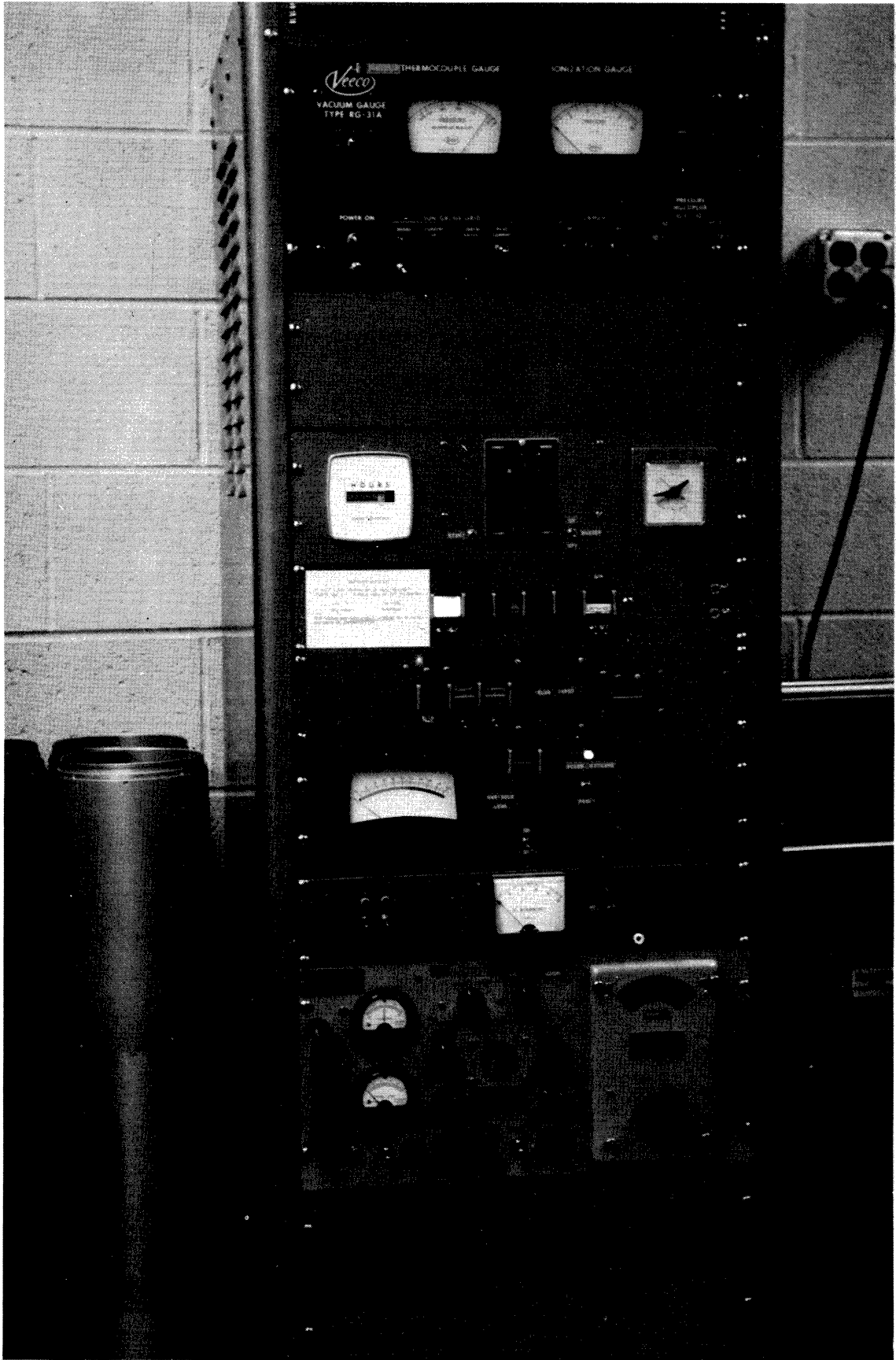


Figure 28. Vacuum system control panel.

UNIVERSITY OF MICHIGAN



3 9015 03026 8018